Bergische Universität Wuppertal

Fachbereich Mathematik und Naturwissenschaften

Lehrstuhl für Angewandte Mathematik
und Numerische Mathematik

Preprint BUW-AMNA 06/05

Roland Pulch, Michael Günther and Stephanie Knorr

Multirate Partial Differential Algebraic Equations for Simulating Radio Frequency Signals

October 2006

http://www.math.uni-wuppertal.de/org/Num/

Multirate Partial Differential Algebraic Equations for Simulating Radio Frequency Signals

Roland Pulch, Michael Günther and Stephanie Knorr

Lehrstuhl für Angewandte Mathematik und Numerische Analysis,
Bergische Universität Wuppertal, Gaußstr. 20, D-42119 Wuppertal, Germany.
Email: `[pulch,guenther,knorr]@math.uni-wuppertal.de`

Abstract

In radio frequency (RF) applications, electric circuits produce signals exhibiting fast oscillations, whereas the amplitude and frequency may change slowly in time. Thus solving a system of differential algebraic equations (DAEs), which describes the circuit's transient behaviour, becomes inefficient, since the fast rate restricts the step sizes in time. A multivariate model is able to decouple the widely separated time scales of RF signals and thus provides an alternative approach. Consequently, a system of DAEs changes into a system of multirate partial differential algebraic equations (MPDAEs). The determination of multivariate solutions allows the exact reconstruction of corresponding time-dependent signals. Hence an efficient numerical simulation is obtained by exploiting the periodicities in fast time scales. We outline the theory of this multivariate approach with respect to the simulation of amplitude as well as frequency modulated signals. Furthermore, a survey of numerical methods for solving the arising problems of MPDAEs is given.

1 Introduction

In many applications, technical systems comprise parts that evolve at largely differing time scales: for example, in vehicle system dynamics, the interaction of catenary and pantograph links the fast mode of the catenary with the relatively slow dynamics of the vehicle [31]; in chip design, often only small subsystems of a chip are active, whereas the largest part is evolving quite slowly or remains nearly inactive [32]. To exploit this multiscale behaviour in time, specialised schemes have been and are currently developed, which do not use a joint step size defined by the fastest mode for the whole system, but employ this multirate potential by treating each subsystem with an appropriate time stepping, see [8] for an overview.

Another source of multiscale behaviour are multitone systems. Here the multirate behaviour cannot be localised at subsystem level, but is spread over the whole system: each function of the solution itself combines a dynamical behaviour at different, usually widely separated time scales. This type of multirate behaviour is typically for radio frequency (RF) circuits, which are in the core of today's telecommunication systems.

In an industrial framework, RF circuits especially and electrical networks in general, are usually modelled by applying the modified nodal approach (MNA) [30]. Written in a compact way, this approach results in the MNA network equations

$$\frac{\mathrm{d}}{\mathrm{d}t}\,\mathbf{q}(\mathbf{x}(t)) = \mathbf{f}(\mathbf{b}(t), \mathbf{x}(t)), \tag{1.1}$$

where the unknown voltages and currents are collected in $\mathbf{x} : \mathbb{R} \to \mathbb{R}^k$, $\mathbf{q} : \mathbb{R}^k \to \mathbb{R}^k$ comprises charges and fluxes, and the right-hand side $\mathbf{f} : \mathbb{R}^s \times \mathbb{R}^k \to \mathbb{R}^k$ contains time-dependent input signals $\mathbf{b} : \mathbb{R} \to \mathbb{R}^s$. As the Jacobian $\partial\mathbf{q}(\mathbf{x})/\partial\mathbf{x}$ is singular in general, one has to deal with differential algebraic equations (DAEs).

This paper aims at giving a survey on how to model and simulate numerically these systems in an appropriate, i.e. fast, robust and reliable way, if the involved signals exhibit a multitone behaviour. Accordingly, a multivariate model can be employed to represent the signals. Hence the differential algebraic system (1.1) is analytically transformed into a singular system of partial differential equations, the multirate partial differential algebraic equations (MPDAEs). The MPDAE system can be solved more efficiently than the original DAE description, since time scales are decoupled.

The paper is organised as follows: in Chapter 2, we deal with systems, which feature a pure amplitude modulation (AM) and thus exhibit constant time rates. We start with a careful discussion of the MPDAE approach based on a multivariate model for amplitude modulated signals and use the specific structure of the MPDAE system to verify the well-posedness of the system. Chapter 3 is devoted to systems with frequency modulation (FM), which do not possess constant time rates. Based on a multivariate model for frequency modulated signals, we consider a warped MPDAE model as generalisation of the approach for amplitude modulated signals. The so-called local frequency function will turn out as some kind of a generalised modelling parameter, which enables different but analytically equivalent descriptions of the RF circuits, provided that some transformation properties are fulfilled. Conditions for an appropriate choice of this modelling parameter can be based on simple boundary conditions or on solving optimisation problems. In each chapter, a second part gives an overview on numerical methods proposed so far in the literature, which can be classified as frequency, time or mixed domain methods. Both chapters are finished by a careful discussion of an illustrative example, the ring modulator and the Colpitt oscillator, respectively. Finally, Chapter 4 concludes the paper and gives an outlook in future research.

2 Model for Constant Frequencies

In this chapter, we consider the case of multitone signals in RF circuits, where the arising time rates are forced by independent inputs and thus are constant. Consequently, the multidimensional model employs constant frequencies for the representation as well as the numerical simulation of such signals.

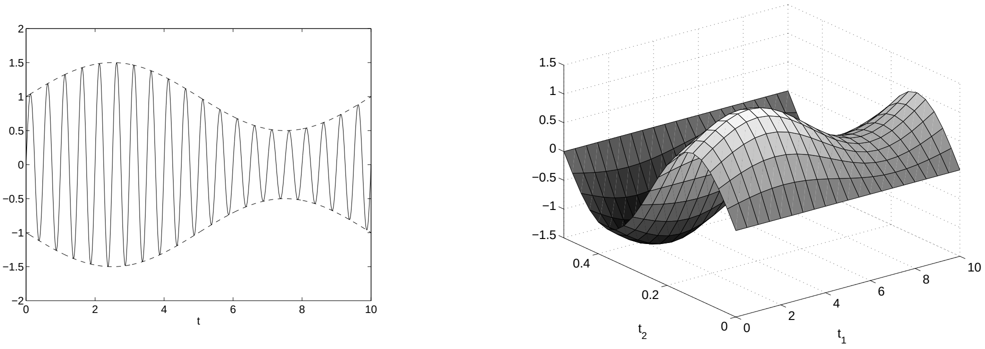

FIGURE 1. Signal x (left) and its multivariate function $\hat{x}$ (right).

2.1 Multidimensional Approach

2.1.1 *Multivariate Model for AM Signals*

The idea to face widely separated time scales is to introduce a corresponding variable to each of them. The multidimensional representation of a signal is then called *multivariate function (MVF)*. A quasiperiodic signal $\mathbf{x} : \mathbb{R} \to \mathbb{C}^k$ with m fundamental frequencies $\omega_l = 2\pi/T_l$, $l = 1, \ldots, m$, can be represented via

$$\mathbf{x}(t) = \sum_{j_1=-\infty}^{\infty} \cdots \sum_{j_m=-\infty}^{\infty} \mathbf{X}_{j_1,\ldots,j_m} \exp(i(j_1\omega_1 + \cdots + j_m\omega_m)\, t), \tag{2.1}$$

where $\mathbf{X}_{j_1,\ldots,j_m} \in \mathbb{C}^k$ and $i = \sqrt{-1}$. This multirate structure leads naturally to the corresponding MVF $\hat{\mathbf{x}} : \mathbb{R}^m \to \mathbb{C}^k$ with

$$\hat{\mathbf{x}}(t_1, \ldots, t_m) = \sum_{j_1=-\infty}^{\infty} \cdots \sum_{j_m=-\infty}^{\infty} \mathbf{X}_{j_1,\ldots,j_m} \exp(i(j_1\omega_1 t_1 + \cdots + j_m\omega_m t_m)). \tag{2.2}$$

Now the time scales are decoupled in the multidimensional model. Moreover, the MVF is periodic in each coordinate direction. The original signal is contained in the MVF and can be reconstructed by $\mathbf{x}(t) = \hat{\mathbf{x}}(t, \ldots, t)$, which follows the diagonal direction. This proceeding is also applicable, if the fundamental frequencies $\omega_1, \ldots, \omega_m$ are commensurable.

For illustration, we introduce a two-tone quasiperiodic signal $x : \mathbb{R} \to \mathbb{R}$,

$$x(t) := \left[1 + \alpha \sin\left(\tfrac{2\pi}{T_1} t\right)\right] \cdot \sin\left(\tfrac{2\pi}{T_2} t\right) \tag{2.3}$$

with $0 < \alpha < 1$, which exhibits amplitude modulation including two different time scales $T_1 > T_2$. Its MVF $\hat{x} : \mathbb{R}^2 \to \mathbb{R}$ is derived as follows:

$$\hat{x}(t_1, t_2) = \left[1 + \alpha \sin\left(\tfrac{2\pi}{T_1} t_1\right)\right] \cdot \sin\left(\tfrac{2\pi}{T_2} t_2\right). \tag{2.4}$$

Fig. 1 shows the signal x and its MVF $\hat{x}$, which is determined in the rectangle $[0, T_1] \times [0, T_2]$. The more the time scales differ ($T_1 \gg T_2$), the more efficient the multidimensional approach becomes, since the structure of the MVF is independent from the ratio T_1/T_2.

In the case of m different time scales with $m - 1$ periodic and one aperiodic scale, we consider envelope-modulated signals

$$\mathbf{x}(t) = \sum_{j_2=-\infty}^{\infty} \cdots \sum_{j_m=-\infty}^{\infty} \mathbf{X}_{j_2,\ldots,j_m}(t) \exp(i(j_2\omega_2 + \cdots + j_m\omega_m)\, t) \tag{2.5}$$

with functions $\mathbf{X}_{j_2,\ldots,j_m} : \mathbb{R} \to \mathbb{C}^k$. Usually, the aperiodic part is the slowest time scale. The MVF is obtained analogously to the quasiperiodic case with $\mathbf{X}_{j_2,\ldots,j_m}$ then depending on t_1. Hence signals of this type can be represented efficiently by the multidimensional approach, too.

2.1.2 *MPDAE Model*

Now we apply the multidimensional signal model to solutions of the differential algebraic network equations (1.1), which have been established in Chapter 1. To determine quasiperiodic solutions (2.1) on the level of the DAEs (1.1), time and frequency domain methods have been introduced in [5] and [34], respectively.

Assuming m different time scales, we introduce MVFs $\hat{\mathbf{x}} : \mathbb{R}^m \to \mathbb{R}^k$ of the unknowns and $\hat{\mathbf{b}} : \mathbb{R}^m \to \mathbb{R}^s$ of the input signals. Considering the DAEs (1.1), Brachtendorf et al. [2] introduced the corresponding *multirate partial differential algebraic equations* (*MPDAEs*)

$$\frac{\partial \mathbf{q}(\hat{\mathbf{x}})}{\partial t_1} + \cdots + \frac{\partial \mathbf{q}(\hat{\mathbf{x}})}{\partial t_m} = \mathbf{f}(\hat{\mathbf{b}}(t_1, \ldots, t_m), \hat{\mathbf{x}}(t_1, \ldots, t_m)). \tag{2.6}$$

Given a solution of the MPDAE (2.6), we can reconstruct a solution of the original DAE (1.1) by

$$\mathbf{x}(t) = \hat{\mathbf{x}}(t, \ldots, t), \tag{2.7}$$

see [2]. To solve the MPDAE, we have to impose boundary conditions, which determine the structure of the obtained solution. If the inputs $\mathbf{b}$ of (1.1) are quasiperiodic, then a quasiperiodic output $\mathbf{x}$ with identical time rates is expected. Looking for an m-tone quasiperiodic solution (2.1) of the DAE, we solve the MPDAE for an m-periodic MVF specifying the boundary conditions

$$\hat{\mathbf{x}}(t_1, \ldots, t_m) = \hat{\mathbf{x}}(t_1 + k_1 T_1, \ldots, t_m + k_m T_m) \quad \text{for all } t_1, \ldots, t_m \in \mathbb{R} \text{ and } k_1, \ldots, k_m \in \mathbb{Z}\,. \tag{2.8}$$

Considering envelope-modulated signals (2.5) with $m-1$ periodic rates and one aperiodic time scale, we solve an initial-boundary value problem

$$\begin{aligned} \hat{\mathbf{x}}(0, t_2, \ldots, t_m) &= \mathbf{h}(t_2, \ldots, t_m) && \text{for all } t_2, \ldots, t_m \in \mathbb{R}, \\ \hat{\mathbf{x}}(t_1, t_2, \ldots, t_m) &= \hat{\mathbf{x}}(t_1, t_2 + k_2 T_2, \ldots, t_m + k_m T_m) && \text{for all } t_1, \ldots, t_m \in \mathbb{R} \\ &&& \text{and } k_2, \ldots, k_m \in \mathbb{Z}\,. \end{aligned} \tag{2.9}$$

The function $\mathbf{h}$ has to be prescribed appropriately. It follows that the reconstructed signal (2.7) depends only on $\mathbf{h}(0, \ldots, 0)$, i.e. for each function $\mathbf{h}$ with $\mathbf{h}(0, \ldots, 0) = \mathbf{x}(0)$, the same solution will be obtained. For a more detailed description of the relation between DAE and MPDAE solutions, we refer to Roychowdhury [29].

In practice, mostly systems comprising exactly two different time scales arise:

$$\frac{\partial \mathbf{q}(\hat{\mathbf{x}})}{\partial t_1} + \frac{\partial \mathbf{q}(\hat{\mathbf{x}})}{\partial t_2} = \mathbf{f}(\hat{\mathbf{b}}(t_1, t_2), \hat{\mathbf{x}}(t_1, t_2)). \tag{2.10}$$

The corresponding biperiodic boundary conditions read

$$\begin{aligned} \hat{\mathbf{x}}(t_1, t_2) &= \hat{\mathbf{x}}(t_1 + T_1, t_2) \quad \text{for all } \ t_1, t_2 \in \mathbb{R}, \\ \hat{\mathbf{x}}(t_1, t_2) &= \hat{\mathbf{x}}(t_1, t_2 + T_2) \quad \text{for all } \ t_1, t_2 \in \mathbb{R}, \end{aligned} \tag{2.11}$$

and the initial-boundary value problem is solved with

$$\begin{aligned} \hat{\mathbf{x}}(0, t_2) &= \mathbf{h}(t_2) \qquad\qquad \text{for all } \ t_2 \in \mathbb{R}, \\ \hat{\mathbf{x}}(t_1, t_2) &= \hat{\mathbf{x}}(t_1, t_2 + T_2) \quad \text{for all } \ t_1, t_2 \in \mathbb{R}. \end{aligned} \tag{2.12}$$

The initial-boundary value problem can be used to determine biperiodic solutions in case of quasiperiodic input signals, too. Accordingly, the problem is solved proceeding in t_1-direction until the solution enters a biperiodic steady state response. This strategy can be seen as a multidimensional generalisation of transient analysis by applying more information about the signal structure. Furthermore, if the input signals are just periodic with one time rate, then the problem (2.12) using two time scales also yields periodic responses of the DAE (1.1). Starting from some initial condition, the MPDAE (2.10) is solved until the solution reaches a periodic signal, i.e. the Fourier coefficients in (2.5) become constant.

Before considering numerical schemes, we investigate the structure of the MPDAE and the well-posedness of the problem.

2.1.3 *Characteristic System of the MPDAE*

The following results are based on the special structure of the MPDAE (2.6) and its inherent partial differential equation (PDE), which have been investigated in [21]. In this paper, we just give a short overview of the basic ideas.

The inherent PDE of system (2.6) is of hyperbolic type, where each component of the system consists of a derivative in direction of the diagonal. Thus the information transport takes place along *characteristic curves*, which are straight lines in diagonal direction. The algebraic constraints in case of DAEs do not affect this information transport and we are able to formulate the characteristic system of (2.6)

$$\begin{aligned} \tfrac{\mathrm{d}}{\mathrm{d}\tau} t_l(\tau) &= 1, \quad l = 1, \ldots, m \\ \tfrac{\mathrm{d}}{\mathrm{d}\tau} \mathbf{q}(\hat{\mathbf{x}}(\tau)) &= \mathbf{f}(\hat{\mathbf{b}}(t_1(\tau), \ldots, t_m(\tau)), \hat{\mathbf{x}}(\tau)). \end{aligned} \tag{2.13}$$

Thereby, the time variables as well as the MVF of the solution depend on a parameter τ. The part corresponding to the time variables can be solved explicitly. Hence we obtain the *characteristic projections*

$$(t_1(\tau), \ldots, t_m(\tau)) = (\tau + c_1, \ldots, \tau + c_m) \quad \text{for arbitrary } \ c_1, \ldots, c_m \in \mathbb{R}. \tag{2.14}$$

The characteristic projections represent a continuum of parallel straight lines in the domain of dependence. Inserting this result in the last equation of the characteristic system (2.13) yields

$$\frac{\mathrm{d}}{\mathrm{d}\tau} \mathbf{q}(\hat{\mathbf{x}}(\tau)) = \mathbf{f}(\hat{\mathbf{b}}(\tau + c_1, \ldots, \tau + c_m), \hat{\mathbf{x}}(\tau)). \tag{2.15}$$

This family of DAE systems describes the transport of information in the system of MPDAEs (2.6) completely.

Due to the hyperbolic structure of the system, Cauchy initial value problems are well-posed provided that initial conditions are consistent. Moreover, the structure can be used to solve multiperiodic boundary value problems numerically, as we will see in Sect. 2.2.

2.1.4 *Well-Posedness of Problems*

To investigate the properties of the MPDAE system (2.6) with respect to algebraic constraints, we have to write the original DAE of the network approach in a more detailed version. Excluding controlled sources, modified nodal analysis [7, 30] leads to the system

$$
\begin{aligned}
A_C\dot{\tilde{\mathbf{q}}} + A_R\mathbf{r}(A_R^\top\mathbf{u}(t),t) + A_L\boldsymbol{\jmath}_L(t) + A_V\boldsymbol{\jmath}_V(t) + A_I\boldsymbol{\imath}(t) \;&=\; \mathbf{0}, && (2.16\,a)\\
\dot{\mathbf{\Phi}} - A_L^\top\mathbf{u}(t) \;&=\; \mathbf{0}, && (2.16\,b)\\
A_V^\top\mathbf{u}(t) - \mathbf{v}(t) \;&=\; \mathbf{0}, && (2.16\,c)\\
\tilde{\mathbf{q}} - \mathbf{q}_C(A_C^\top\mathbf{u}(t),t) \;&=\; \mathbf{0}, && (2.16\,d)\\
\mathbf{\Phi} - \mathbf{\Phi}_L(\boldsymbol{\jmath}_L(t),t) \;&=\; \mathbf{0}. && (2.16\,e)
\end{aligned}
$$

Thereby, we have the incidence matrices A_C, A_R, A_L and A_V, A_I belonging to capacitive, resistive, inductive parts of the network and to branches with independent voltage and current sources, respectively. Correspondingly, we denote the functions $\tilde{\mathbf{q}}$ for charges, $\mathbf{\Phi}$ for fluxes, $\mathbf{r}$ for resistances, $\boldsymbol{\imath}$ for current and $\mathbf{v}$ for voltage sources. The state variables $(\mathbf{u},\boldsymbol{\jmath}_L,\boldsymbol{\jmath}_V)^\top$ are node potentials and currents through inductances and voltage sources. To shorten notation we will skip the time-dependence of the state variables from now on.

In [14], the multidimensional signal model is applied to the system (2.16) and the resulting "detailed version" of an MPDAE is resolved for structural properties. For this purpose, the MPDAE is split into a semi-explicit system of PDEs and algebraic equations. This is done with the use of orthogonal projectors following Estèvez Schwarz and Tischendorf [6], who carry out the splitting for the original network-DAE (2.16).

As the derivation of the MPDAE's semi-explicit formulation is rather technical and lengthy, we show an equivalent approach, where we start from the semi-explicit DAE-formulation due to [6] and then introduce the multidimensional signal model. Thereby, we do not have to deal with the various projectors, which are needed to split the equations, but we can focus on the transfer by MVFs.

The relation of index properties of the differential algebraic network equations and topological conditions of the circuit have also been investigated by Tischendorf [33]. The network-DAE (2.16) has differential index 1, if the following two topological conditions are fulfilled:

T1: There are no cutsets consisting of inductances and/or current sources only: $\ker(A_C,A_R,A_V)^\top = \{\mathbf{0}\}$.

T2: There are no loops consisting of only capacitances and at least one voltage source: $\ker Q_C^\top A_V = \{\mathbf{0}\}$.

In [6], the authors prove that the system (2.16) can then be written in the semi-explicit form

$$\begin{aligned}P_C\dot{\mathbf{u}} \;&=\; -\,H_1^{-1}(A_C^\top\mathbf{u},t)P_C^\top\Big[A_C\tfrac{\partial}{\partial t}\mathbf{q}_C(A_C^\top\mathbf{u},t)\\&\qquad +A_R\mathbf{r}(A_R^\top\mathbf{u},t)+A_L\boldsymbol{\jmath}_L+A_V\boldsymbol{\jmath}_V+A_I\boldsymbol{\imath}(t)\Big], &(2.17\,a)\\ \dot{\boldsymbol{\jmath}}_L \;&=L^{-1}(\boldsymbol{\jmath}_L,t)\left(A_L^\top\mathbf{u}-\tfrac{\partial}{\partial t}\boldsymbol{\Phi}_L(\boldsymbol{\jmath}_L,t)\right), &(2.17\,b)\\ \mathbf{0}\;&=Q_C^\top\left[A_R\mathbf{r}(A_R^\top\mathbf{u},t)+A_L\boldsymbol{\jmath}_L+A_V\boldsymbol{\jmath}_V+A_I\boldsymbol{\imath}(t)\right], &(2.17\,c)\\ \mathbf{0}\;&=A_V^\top\mathbf{u}-\mathbf{v}(t). &(2.17\,d)\end{aligned}$$

This is done with the help of the orthogonal projectors Q_C onto the kernel of $A_C^\top$, and P_C such that $Q_C+P_C=I$. The capacitance and inductance matrices

$$C(\mathbf{w},t):=\frac{\partial\mathbf{q}_C(\mathbf{w},t)}{\partial\mathbf{w}}\quad\text{and}\quad L(\mathbf{w},t):=\frac{\partial\boldsymbol{\Phi}_L(\mathbf{w},t)}{\partial\mathbf{w}} \tag{2.18}$$

as well as the matrix

$$H_1(A_C^\top\mathbf{u},t):=A_CC(A_C^\top\mathbf{u},t)A_C^\top+Q_C^\top Q_C \tag{2.19}$$

are positive definite. Thus the system (2.17) defines differential equations for $P_C\mathbf{u}$ and $\boldsymbol{\jmath}_L$ and two constraints, which can be resolved for the algebraic variables $Q_C\mathbf{u}$ and $\boldsymbol{\jmath}_V$.

We apply the multidimensional signal model for the biperiodic case of two different time scales and represent each time-dependent function occurring in (2.17) by its MVF. Moreover, we introduce

$$\hat{C}(\mathbf{w},t_1,t_2):=\frac{\partial\hat{\mathbf{q}}_C(\mathbf{w},t_1,t_2)}{\partial\mathbf{w}}\quad\text{and}\quad\hat{L}(\mathbf{w},t_1,t_2):=\frac{\partial\hat{\boldsymbol{\Phi}}_L(\mathbf{w},t_1,t_2)}{\partial\mathbf{w}}, \tag{2.20}$$

which are assumed to be positive definite with a globally bounded inverse on the domain $[0,T_1]\times[0,T_2]$ defined by the time scales.

Altogether, we obtain the semi-explicit MPDAE system

$$\begin{aligned}\frac{\partial P_C\hat{\mathbf{u}}}{\partial t_1}+\frac{\partial P_C\hat{\mathbf{u}}}{\partial t_2}\;&=\;-\hat{H}_1^{-1}(A_C^\top\hat{\mathbf{u}},t_1,t_2)P_C^\top\Big[A_C\left(\tfrac{\partial\hat{\mathbf{q}}_C}{\partial t_1}+\tfrac{\partial\hat{\mathbf{q}}_C}{\partial t_2}\right)(A_C^\top\hat{\mathbf{u}},t_1,t_2)\\&\qquad+A_R\hat{\mathbf{r}}(A_R^\top\hat{\mathbf{u}},t_1,t_2)+A_L\hat{\boldsymbol{\jmath}}_L+A_V\hat{\boldsymbol{\jmath}}_V+A_I\hat{\boldsymbol{\imath}}(t_1,t_2)\Big], &(2.21\,a)\\ \frac{\partial\hat{\boldsymbol{\jmath}}_L}{\partial t_1}+\frac{\partial\hat{\boldsymbol{\jmath}}_L}{\partial t_2}\;&=\;\hat{L}^{-1}(\hat{\boldsymbol{\jmath}}_L,t_1,t_2)\left(A_L^\top\hat{\mathbf{u}}-\left(\tfrac{\partial\hat{\boldsymbol{\Phi}}_L}{\partial t_1}+\tfrac{\partial\hat{\boldsymbol{\Phi}}_L}{\partial t_2}\right)(\hat{\boldsymbol{\jmath}}_L,t_1,t_2)\right), &(2.21\,b)\\ \mathbf{0}\;&=\;Q_C^\top\left[A_R\hat{\mathbf{r}}(A_R^\top\hat{\mathbf{u}},t_1,t_2)+A_L\hat{\boldsymbol{\jmath}}_L+A_V\hat{\boldsymbol{\jmath}}_V+A_I\hat{\boldsymbol{\imath}}(t_1,t_2)\right], &(2.21\,c)\\ \mathbf{0}\;&=\;A_V^\top\hat{\mathbf{u}}-\hat{\mathbf{v}}(t_1,t_2), &(2.21\,d)\end{aligned}$$

where again the matrix

$$\hat{H}_1(A_C^\top\hat{\mathbf{u}},t_1,t_2):=A_C\hat{C}(A_C^\top\hat{\mathbf{u}},t_1,t_2)A_C^\top+Q_C^\top Q_C \tag{2.22}$$

is positive definite by construction. The two constraints (2.21 c) and (2.21 d) are resolvable for the algebraic variables $Q_C\hat{\mathbf{u}}$ and $\hat{\boldsymbol{\jmath}}_V$, iff the topological conditions T1 and T2 hold. Thus, similar to the case of DAEs, the MPDAE-formulation of (2.16) is represented by a PDE on a manifold, which can be written as a so called "underlying PDE", cf. [14].

If one of the topological conditions is violated, the network-DAE (2.16) is of index 2.

In this case, the system can also be written in a semi-explicit form, where the algebraic variables of (2.17) are split into index-1 and index-2 variables using further orthogonal projectors. Applying the multidimensional signal model yields again a semi-explicit MPDAE, which can also be derived starting from the MPDAE-formulation of (2.16) and then splitting the MVFs of the network variables via the same orthogonal projectors as for the DAE system.

Thus, in both index-1 and index-2 cases of the network-DAE, the corresponding MPDAE inherits all the structural properties of the original system. Moreover, when looking at the characteristic system (2.15), we also retrieve the structure of the original network-DAE (2.16). Due to the particular structure, it is naturally to assign index concepts for DAEs to the MPDAE system. Therefore we do not expect additional stability problems, when solving the network equations via the multidimensional approach.

For the general DAE-formulation (1.1), a comparison to (2.16) yields

$$\mathbf{x} := (\tilde{\mathbf{q}}, \mathbf{\Phi}, \mathbf{u}, \boldsymbol{\jmath}_L, \boldsymbol{\jmath}_V)^\top, \quad \mathbf{q}(\mathbf{x}) := (A_C\tilde{\mathbf{q}}, \mathbf{\Phi}, 0, 0, 0)^\top \tag{2.23}$$

and the remaining terms comprise the right-hand side with the time-dependent input signals. Thus the network-DAEs (2.16) represent a special case of (1.1), where a linear function $\mathbf{q}$ arises. Furthermore, the general form (1.1) includes a broad class of DAEs obtained by other mathematical models of electric circuits than MNA, see [13] for examples. For shortness, we use the compact formulation (1.1) to outline numerical methods in the following sections.

2.2 Numerical Methods

In this section, we describe numerical methods for solving initial-boundary value problems (2.9) as well as multiperiodic boundary value problems (2.8) of the MPDAE system. Thereby, we restrict to the case of two time scales, since generalisations to three or more time variables are straightforward. Thus we consider the MPDAE (2.10) in the following.

2.2.1 *Frequency Domain Methods*

Brachtendorf et al. [2] introduced a method for determining biperiodic solutions according to (2.11) purely in frequency domain. Therefore both time scales have to be periodic, since a representation using Fourier coefficients is applied for each variable. This strategy can be seen as a multidimensional generalisation of the harmonic balance technique.

The approximation is obtained via a Galerkin approach. The MPDAE implies the definition of the residual

$$\mathbf{r}(t_1, t_2) := \frac{\partial \mathbf{q}(\hat{\mathbf{x}})}{\partial t_1}(t_1, t_2) + \frac{\partial \mathbf{q}(\hat{\mathbf{x}})}{\partial t_2}(t_1, t_2) - \mathbf{f}(\hat{\mathbf{b}}(t_1, t_2), \hat{\mathbf{x}}(t_1, t_2)) \tag{2.24}$$

and thus the corresponding weak formulation reads

$$\frac{1}{T_1 T_2} \int_0^{T_1} \int_0^{T_2} \mathbf{r}(t_1, t_2) \cdot \overline{\mathbf{\Psi}(t_1, t_2)} \, \mathrm{d}t_2 \, \mathrm{d}t_1 = \mathbf{0} \tag{2.25}$$

for all test functions $\mathbf{\Psi} : \mathbb{R}^2 \to \mathbb{C}^k$. The integration, multiplication and complex conjugation operate in each component $l = 1, \ldots, k$ separately here. The unknown solution is approximated by a finite sum of two-dimensional trigonometric polynomials

$$\hat{\mathbf{x}}(t_1, t_2) \doteq \sum_{j_1=-p_1}^{p_1} \sum_{j_2=-p_2}^{p_2} \hat{\mathbf{X}}_{j_1,j_2} \exp\left(i(\omega_1 j_1 t_1 + \omega_2 j_2 t_2)\right) \tag{2.26}$$

with $\hat{\mathbf{X}}_{j_1,j_2} \in \mathbb{C}^k$ and frequencies $\omega_l = 2\pi/T_l$ for $l = 1, 2$. This approximation is biperiodic due to its construction. The basis functions used in the sum (2.26) form an orthogonal system with respect to the sesquilinear form corresponding to (2.25). Let $\hat{\mathbf{Q}}_{j_1,j_2}$ and $\hat{\mathbf{F}}_{j_1,j_2}$ be the according Fourier coefficients of the biperiodic functions $\mathbf{q}(\hat{\mathbf{x}})$ and $\mathbf{f}(\hat{\mathbf{b}}, \hat{\mathbf{x}})$, respectively. Hence these values depend on all unknowns $\hat{\mathbf{X}} := (\hat{\mathbf{X}}_{j_1,j_2})$. Now the partial derivatives can be evaluated explicitly

$$\begin{aligned}
&\frac{\partial \mathbf{q}(\hat{\mathbf{x}})}{\partial t_1}(t_1, t_2) + \frac{\partial \mathbf{q}(\hat{\mathbf{x}})}{\partial t_2}(t_1, t_2) \\
&\doteq \sum_{j_1=-p_1}^{p_1} \sum_{j_2=-p_2}^{p_2} i(\omega_1 j_1 + \omega_2 j_2) \hat{\mathbf{Q}}_{j_1,j_2}(\hat{\mathbf{X}}) \exp\left(i(\omega_1 j_1 t_1 + \omega_2 j_2 t_2)\right).
\end{aligned} \tag{2.27}$$

Thus we define the coefficients

$$\hat{\mathbf{H}}_{j_1,j_2}(\hat{\mathbf{X}}) := i(\omega_1 j_1 + \omega_2 j_2) \hat{\mathbf{Q}}_{j_1,j_2}(\hat{\mathbf{X}}) - \hat{\mathbf{F}}_{j_1,j_2}(\hat{\mathbf{X}}). \tag{2.28}$$

Following the Galerkin approach, we employ the test functions

$$\mathbf{\Psi}(t_1, t_2) = \mathbf{e} \cdot \exp\left(i(\omega_1 j_1^* t_1 + \omega_2 j_2^* t_2)\right) \tag{2.29}$$

for $j_1^* = -p_1, \ldots, p_1,\ j_2^* = -p_2, \ldots, p_2$, where $\mathbf{e} \in \mathbb{C}^k$ denotes $\mathbf{e} := (1, \ldots, 1)^\top$. Inserting the residual, which depends on the coefficients (2.28), and the test functions in (2.25) yields the equations

$$\begin{aligned}
&\frac{1}{T_1 T_2} \int_0^{T_1} \int_0^{T_2} \sum_{j_1=-p_1}^{p_1} \sum_{j_2=-p_2}^{p_2} \hat{\mathbf{H}}_{j_1,j_2}(\hat{\mathbf{X}}) \exp\left(i\tilde{\omega}(t_1, t_2)\right)\, \mathrm{d}t_2\, \mathrm{d}t_1 = \mathbf{0} \\
&\text{with} \quad \tilde{\omega}(t_1, t_2) := \omega_1 (j_1 - j_1^*) t_1 + \omega_2 (j_2 - j_2^*) t_2
\end{aligned} \tag{2.30}$$

for $j_1^* = -p_1, \ldots, p_1,\ j_2^* = -p_2, \ldots, p_2$. If we interchange integration and summation, then the orthogonality of the basis functions implies

$$\hat{\mathbf{H}}_{j_1,j_2}(\hat{\mathbf{X}}) = \mathbf{0} \quad \text{for} \quad j_1 = -p_1, \ldots, p_1,\ j_2 = -p_2, \ldots, p_2. \tag{2.31}$$

Hence we obtain a nonlinear system of $(2p_1 + 1)(2p_2 + 1)k$ equations for the unknown Fourier coefficients in (2.26). Methods of Newton type yield a corresponding approximation of the involved coefficients. The efficient evaluation of the nonlinear system and its Jacobian matrix demands discrete Fourier transformations and their inverse mappings. Since we consider solutions $\hat{\mathbf{x}} : \mathbb{R}^2 \to \mathbb{R}^k$, an equivalent real-valued formulation of the approach leads to a nonlinear system for the real degrees of freedom only.

The above method has been successfully used in numerical simulations of according electric circuits, see [2]. The frequency domain technique is efficient, if the time scales exhibit a nearly linear behaviour, i.e. arising functions are similar to harmonic oscillations. However, strongly nonlinear functions in the MPDAE system may demand a huge number of coefficients in the sum (2.26) to obtain sufficiently accurate approximations. Hence the pure frequency domain method becomes inefficient. In this case, time domain techniques offer an adequate alternative.

2.2.2 *Time Domain Methods*

In time domain, techniques can be applied for solving initial-boundary value problems (2.12) as well as biperiodic boundary value problems (2.11). A simple approach to obtain approximations of biperiodic solutions of the MPDAE (2.10) consists in a finite difference method. Thereby, the partial derivatives are replaced by difference formulae applying values of the solution on a grid in time domain. For simplicity, we apply a uniform grid with the points

$$(t_{1,j_1}, t_{2,j_2}) := ((j_1 - 1)h_1, (j_2 - 1)h_2), \quad \text{where } h_1 := \tfrac{T_1}{n_1} \text{ and } h_2 := \tfrac{T_2}{n_2} \tag{2.32}$$

for $j_1 = 1, \ldots, n_1$ and $j_2 = 1, \ldots, n_2$. The values $\hat{\mathbf{x}}_{j_1,j_2} := \hat{\mathbf{x}}(t_{1,j_1}, t_{2,j_2}) \in \mathbb{R}^k$ are unknown. If we substitute the partial derivatives by symmetric differences, for example, then the nonlinear equations

$$\begin{aligned} & \tfrac{1}{2h_1}\left[\mathbf{q}(\hat{\mathbf{x}}_{j_1+1,j_2}) - \mathbf{q}(\hat{\mathbf{x}}_{j_1-1,j_2})\right] + \tfrac{1}{2h_2}\left[\mathbf{q}(\hat{\mathbf{x}}_{j_1,j_2+1}) - \mathbf{q}(\hat{\mathbf{x}}_{j_1,j_2-1})\right] \\ = \; & \mathbf{f}(\hat{\mathbf{b}}(t_{1,j_1}, t_{2,j_2}), \hat{\mathbf{x}}_{j_1,j_2}) \end{aligned} \tag{2.33}$$

for $j_1 = 1, \ldots, n_1$ and $j_2 = 1, \ldots, n_2$ arise. The values $\hat{\mathbf{x}}_{j_1,j_2}$ for $j_1 = 0, n_1 + 1$ and $j_2 = 0, n_2 + 1$, which are situated outside the grid, are identified with the solution inside the grid using the periodicities. Hence a nonlinear system of $n_1 n_2 k$ equations for $n_1 n_2 k$ unknowns arises. If the system exhibits a unique solution, methods of Newton type can be applied to obtain an according approximation. Finite difference methods have been successfully used for analysing RF circuits, see [18, 22, 29].

Considering initial-boundary value problems (2.12), techniques based on semidiscretisation are feasible. Consequently, just one partial derivative in (2.10) is replaced by a difference formula and thus a system of DAEs for the resulting approximation arises. Two types of semidiscretisation techniques exist, which correspond to the method of lines and the Rothe method in case of parabolic PDEs with initial-boundary conditions.

Firstly, we consider the technique performing similar to the method of lines. The arising unknown functions are

$$\tilde{\mathbf{x}}_{j_2}(t_1) := \hat{\mathbf{x}}(t_1, (j_2 - 1)h_2) \quad \text{with } h_2 := \tfrac{T_2}{n_2} \quad \text{for } j_2 = 1, \ldots, n_2. \tag{2.34}$$

Now the partial derivative with respect to the second time scale is replaced by a difference formula. For example, using symmetric differences again, we obtain the approximative systems

$$\frac{\mathrm{d}\mathbf{q}(\tilde{\mathbf{x}}_{j_2})}{\mathrm{d}t_1}(t_1) = \mathbf{f}(\hat{\mathbf{b}}(t_1, (j_2 - 1)h_2), \tilde{\mathbf{x}}_{j_2}(t_1)) - \tfrac{1}{2h_2}\left[\mathbf{q}(\tilde{\mathbf{x}}_{j_2+1}(t_1)) - \mathbf{q}(\tilde{\mathbf{x}}_{j_2-1}(t_1))\right] \tag{2.35}$$

for $j_2 = 1, \ldots, n_2$. The periodicity of the second time scale allows the two identifications $\tilde{\mathbf{x}}_0 = \tilde{\mathbf{x}}_{n_2}$ and $\tilde{\mathbf{x}}_{n_2+1} = \tilde{\mathbf{x}}_1$. The condition (2.12) yields according initial values at $t_1 = 0$. Thus we obtain an initial value problem of $n_2 k$ DAEs for the unknown approximations (2.34).

Secondly, we act like in a Rothe method, i.e. we discretise the derivative with respect to the first time scale. Using equidistant step size h_1, the unknown approximations read

$$\tilde{\mathbf{x}}_{j_1}(t_2) := \hat{\mathbf{x}}((j_1 - 1)h_1, t_2) \quad \text{for } \ j_1 = 1, 2, 3, \ldots \ . \tag{2.36}$$

For simplicity, applying a difference formula of first order, we achieve the systems

$$\frac{\mathrm{d}\mathbf{q}(\tilde{\mathbf{x}}_{j_1})}{\mathrm{d}t_2}(t_2) = \mathbf{f}(\hat{\mathbf{b}}((j_1 - 1)h_1, t_2), \tilde{\mathbf{x}}_{j_1}(t_2)) - \tfrac{1}{h_1}\left[\mathbf{q}(\tilde{\mathbf{x}}_{j_1}(t_2)) - \mathbf{q}(\tilde{\mathbf{x}}_{j_1 - 1}(t_2))\right] \tag{2.37}$$

for $j_1 = 2, 3, \ldots$, where the periodicity of the second time scale implies the boundary conditions $\tilde{\mathbf{x}}_{j_1}(0) = \tilde{\mathbf{x}}_{j_1}(T_2)$ for each j_1. The initial conditions from (2.12) determine the starting function $\tilde{\mathbf{x}}_1$ at $t_1 = 0$. Hence this approach yields a sequence of boundary value problems of k DAEs, which have to be solved successively. In later steps, BDF (backward difference formula) schemes of higher order can be used in the semidiscretisation to improve the accuracy.

Furthermore, we can apply the presented techniques based on semidiscretisation to solve the biperiodic problem (2.11), too. In the first approach, the periodicity in t_1 yields a boundary value problem of the DAE systems (2.35) specified by

$$\tilde{\mathbf{x}}_{j_2}(0) = \tilde{\mathbf{x}}_{j_2}(T_1) \quad \text{for all } \ j_2 = 1, \ldots, n_2. \tag{2.38}$$

This periodic problem can be solved by methods described in [16], for example. In the second strategy, the periodicity in t_1 just imposes

$$\tilde{\mathbf{x}}_1(t_2) = \tilde{\mathbf{x}}_{n_1}(t_2) \quad \text{for all } \ t_2 \in [0, T_2], \quad \text{where } \ h_1 := \tfrac{T_1}{n_1}. \tag{2.39}$$

Since the approximation $\tilde{\mathbf{x}}_{n_1}$ is computed starting from $\tilde{\mathbf{x}}_1$, a condition for the unknown initial values of the biperiodic solution arises. Using this approach corresponds to a hierarchical solution of boundary value problems. We try to satisfy the outer condition (2.39) iteratively, whereas we consider the successive inner problems (2.37) to evaluate the outer condition. Numerical results using the latter approach are presented in [21, 29], for example.

Moreover, the transport of information in the MPDAE system can be used to construct methods of characteristics. Considering the initial-boundary value problem (2.12), we apply a discretisation of the initial manifold. For example, using equidistant step sizes yields the points

$$(t_1, t_2) = (0, (j_2 - 1)h_2) \quad \text{for } \ h_2 := \tfrac{T_2}{n_2} \quad \text{and } \ j_2 = 1, \ldots, n_2. \tag{2.40}$$

A unique characteristic projection runs through each point. Hence the systems according to (2.15) with $\tilde{\mathbf{x}}_{j_2}(\tau) := \hat{\mathbf{x}}(\tau, \tau + (j_2 - 1)h_2)$ are

$$\frac{\mathrm{d}\mathbf{q}(\tilde{\mathbf{x}}_{j_2})}{\mathrm{d}\tau}(\tau) = \mathbf{f}(\hat{\mathbf{b}}(\tau, \tau + (j_2 - 1)h_2), \tilde{\mathbf{x}}_{j_2}(\tau)) \quad \text{for } \ j_2 = 1, \ldots, n_2. \tag{2.41}$$

Each DAE system can be solved separately for $\tau \in [0, T_1]$, where the end point T_1 is not necessarily a period. The condition (2.12) defines the initial values of the integration. Moreover, the resulting functions represent exact values of the corresponding solution. However, solving a system of the form (2.41) in the complete time interval $[0, T_1]$ for some $T_1 \gg T_2$ demands the same computational effort than an initial value problem of the original DAE (1.1), which shall be avoided due to the huge number of oscillations. For example, if $T_1 \approx qT_2$ with $q \gg 1$ holds, then $n_2 q$ oscillations have to be resolved.

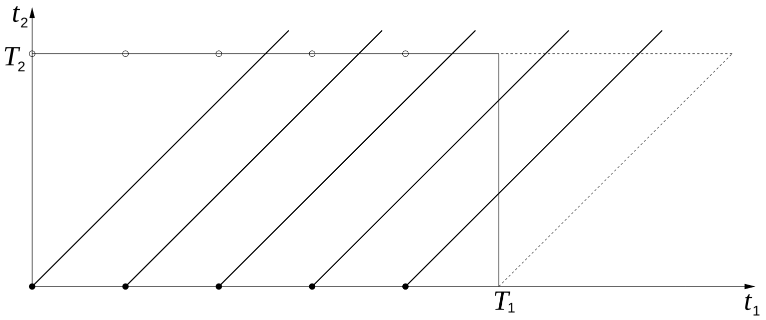

FIGURE 2. Characteristic projections of MPDAE in domain of dependence.

Hence this approach is drastically inefficient for solving initial-boundary value problems, although it is feasible.

Nevertheless, an efficient method of characteristics arises in case of biperiodic boundary value problems. Thereby, we exploit that the biperiodic solution is uniquely defined by its initial values on the manifold $\{(t_1, t_2) \in \mathbb{R}^2 : t_2 = 0\}$, too. Thus the initial points

$$(t_1, t_2) = ((j_1 - 1)h_1, 0) \quad \text{for} \;\; h_1 := \tfrac{T_1}{n_1} \quad \text{and} \;\; j_1 = 1, \ldots, n_1 \tag{2.42}$$

are used. The corresponding systems (2.15) with $\tilde{\mathbf{x}}_{j_1}(\tau) := \hat{\mathbf{x}}(\tau + (j_1 - 1)h_1, \tau)$ read

$$\frac{\mathrm{d}\mathbf{q}(\tilde{\mathbf{x}}_{j_1})}{\mathrm{d}\tau}(\tau) = \mathbf{f}(\hat{\mathbf{b}}(\tau + (j_1 - 1)h_1, \tau), \tilde{\mathbf{x}}_{j_1}(\tau)) \quad \text{for} \;\; j_1 = 1, \ldots, n_1. \tag{2.43}$$

Now the advantage is that each system has to be solved only for $\tau \in [0, T_2]$. Since we assume that $T_1 \gg T_2$, just n_1 oscillations have to be captured in each solution of an initial value problem corresponding to the n_1 subsystems (2.43). Again the systems can be solved separately.

The initial values of the biperiodic solution are unknown a priori. The following strategy can be used to determine these quantities. The periodicity in the first time scale is satisfied via an identification at the boundaries. The periodicity in the second time scale demands

$$\tilde{\mathbf{x}}_{j_1}(0) = \hat{\mathbf{x}}((j_1 - 1)h_1, 0) = \hat{\mathbf{x}}((j_1 - 1)h_1, T_2). \tag{2.44}$$

A unique characteristic projection runs through each initial point, sketched in Fig. 2. Solving the systems (2.43) with initial values from the biperiodic solution yields final values on the line $t_2 = T_2$. We apply these values to interpolate the solution in the points $((j_1 - 1)h_1, T_2)$ for $j_1 = 1, \ldots, n_1$. The periodicity in the first time variable allows to shift the final values for approximating all given points. Considering (2.44), we obtain the linear boundary conditions

$$(\tilde{\mathbf{x}}_1(0), \ldots, \tilde{\mathbf{x}}_{n_1}(0))^\top = \mathcal{B}(\tilde{\mathbf{x}}_1(T_2), \ldots, \tilde{\mathbf{x}}_{n_1}(T_2))^\top, \tag{2.45}$$

where $\mathcal{B} \in \mathbb{R}^{n_1 k \times n_1 k}$ represents a constant matrix depending on the used interpolation scheme. Alternatively, a similar condition can be constructed by interpolating the final values of the integration using the initial points. Hence a boundary value problem of the $n_1 k$ DAEs (2.43) arises. Solving the problem (2.43),(2.45) yields an approximation of the biperiodic solution in the according parallelogram, see Fig. 2. Using the periodicities, we can interpolate an approximation everywhere. The boundary value problem of DAEs can be solved by shooting methods or finite difference methods, for example.

The efficiency of this approach results from applying the specific structure of the hyperbolic PDAE system. The separate characteristic systems (2.43) are only coupled by the boundary conditions (2.45). In contrast, a finite difference method based on a uniform grid performs an unnecessary strong coupling in both coordinate directions. Thus the computational effort of the method of characteristics is much lower in comparison to standard techniques. For example, a comparison between finite difference methods using on the one hand a uniform grid and on the other hand a characteristic grid is given in [22]. Furthermore, the method of characteristics features an inherent potential for parallelism, see [23]. Even applied to circuits including digital-like signal structures, the method of characteristics achieves efficient numerical simulations, see [15].

2.2.3 *Mixed Domain Methods*

In Sect. 2.2.1, a pure frequency domain method is sketched, which is efficient for mildly nonlinear functions in the MPDAE. Otherwise, time domain methods have to be preferred. In some applications, the fast time scale behaves nearly linear, whereas strong nonlinearities arise in the slow part. An early idea of Ngoya and Larchevegue [20] was to transform only the second time scale, which is always assumed to be periodic, into frequency domain. This approach produces the expansion

$$\hat{\mathbf{x}}(t_1, t_2) \doteq \sum_{j_2=-p_2}^{p_2} \hat{\mathbf{X}}_{j_2}(t_1) \exp\left(i\omega_2 j_2 t_2\right) \tag{2.46}$$

with $\hat{\mathbf{X}}_{j_2} : \mathbb{R} \to \mathbb{C}^k$ and $\omega_2 := 2\pi/T_2$. Let $\hat{\mathbf{Q}}_{j_2}(t_1)$ and $\hat{\mathbf{F}}_{j_2}(t_1)$ be the Fourier coefficients of the periodic functions $\mathbf{q}(\hat{\mathbf{x}}(t_1,\cdot))$ and $\mathbf{f}(\hat{\mathbf{b}}(t_1,\cdot), \hat{\mathbf{x}}(t_1,\cdot))$, respectively. These values depend on the unknown functions $\hat{\mathbf{X}} := (\hat{\mathbf{X}}_{j_2}(t_1))$ in (2.46). Following a Galerkin approach similar to the procedure in Sect. 2.2.1, we obtain the relation

$$\sum_{j_2=-p_2}^{p_2} \left[\frac{\mathrm{d}\hat{\mathbf{Q}}_{j_2}(\hat{\mathbf{X}})}{\mathrm{d}t_1}(t_1) + i\omega_2 j_2 (\hat{\mathbf{Q}}_{j_2}(\hat{\mathbf{X}}))(t_1) - (\hat{\mathbf{F}}_{j_2}(\hat{\mathbf{X}}))(t_1) \right] \exp\left(i\omega_2 j_2 t_2\right) = \mathbf{0}. \tag{2.47}$$

Since the arising basis functions are orthogonal, we achieve the conditions

$$\frac{\mathrm{d}\hat{\mathbf{Q}}_{j_2}(\hat{\mathbf{X}})}{\mathrm{d}t_1}(t_1) = (\hat{\mathbf{F}}_{j_2}(\hat{\mathbf{X}}))(t_1) - i\omega_2 j_2 (\hat{\mathbf{Q}}_{j_2}(\hat{\mathbf{X}}))(t_1) \quad \text{for } j_2 = -p_2, \ldots, p_2 \,, \tag{2.48}$$

which represents a system of DAEs for the $(2p_2+1)k$ unknown functions $\hat{\mathbf{X}}_{j_2}$. An equivalent real-valued formulation can be achieved, too. Now we are able to use time domain methods for solving this system. Such mixed techniques are feasible, since the time scales are decoupled. Thus we can tailor our method to the behaviour of the separate time variables and a mixed time-frequency domain scheme arises. The initial-boundary value problem (2.12) yields an initial value problem of the resulting DAEs (2.48). A modification of this MPDAE approach has been used in [1, 4] to determine periodic responses of autonomous DAEs (1.1) as well as their a priori unknown periods. On the other hand, the biperiodic boundary value problem (2.11) implies a periodic boundary value problem for the DAEs (2.48). Corresponding numerical simulations are given in [3, 28, 29].

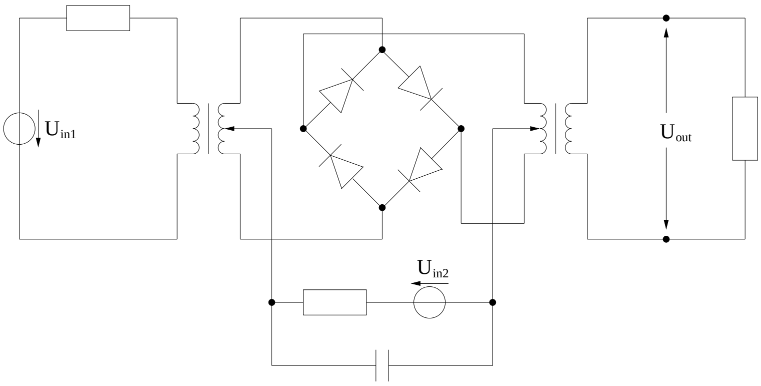

FIGURE 3. Circuit diagram of the ring modulator.

In the discussed approach, we have performed the transformation in frequency domain first and then we want to apply time domain schemes. Vice versa, mixed methods also arise by considering the scheme (2.37), which is produced by a semidiscretisation in time domain. The according sequence of periodic boundary value problems of DAEs can be solved by harmonic balance, too, i.e. a method in frequency domain. Furthermore, the periodic boundary value problem of the DAEs (2.35) allows the use of frequency domain methods, which may be advantageous in case of a mildly nonlinear slow time scale.

2.3 Illustrative Example: Ring Modulator

As example for a numerical simulation using the MPDAE model, we consider the ring modulator. Fig. 3 shows the corresponding circuit diagram. The ring modulator performs a multiplicative mixture of two independent input signals. A mathematical model of the circuit was introduced by Horneber [12]. Thereby, an artifical capacitance C_S is added. Consequently, a system of ordinary differential equations (ODEs) for seven node voltages and eight branch currents arises:

$$\begin{aligned}
C\dot{U}_1 &= I_1 - I_3/2 + I_4/2 + I_7 - U_1/R \\
C\dot{U}_2 &= I_2 - I_5/2 + I_6/2 + I_8 - U_2/R \\
C_S\dot{U}_3 &= I_3 - d(U_{D1}) + d(U_{D4}) \\
C_S\dot{U}_4 &= -I_4 + d(U_{D2}) - d(U_{D3}) \\
C_S\dot{U}_5 &= I_5 + d(U_{D1}) - d(U_{D3}) \\
C_S\dot{U}_6 &= -I_6 - d(U_{D2}) + d(U_{D4}) \\
C_P\dot{U}_7 &= -U_7/R_P + d(U_{D1}) + d(U_{D2}) - d(U_{D3}) - d(U_{D4}) \\
L_H\dot{I}_1 &= -U_1 \\
L_H\dot{I}_2 &= -U_2 \\
L_{S2}\dot{I}_3 &= U_1/2 - U_3 - R_{G2}I_3 \\
L_{S3}\dot{I}_4 &= -U_1/2 + U_4 - R_{G3}I_4 \\
L_{S2}\dot{I}_5 &= U_2/2 - U_5 - R_{G2}I_5 \\
L_{S3}\dot{I}_6 &= -U_2/2 + U_6 - R_{G3}I_6 \\
L_{S1}\dot{I}_7 &= -U_1 + U_{\mathrm{IN1}} - (R_J + R_{G1})I_7 \\
L_{S1}\dot{I}_8 &= -U_2 - (R_C + R_{G1})I_8.
\end{aligned} \tag{2.49}$$

In this system, the following abbreviations for the voltages corresponding to the diodes are used:

$$\begin{aligned} U_{D1} &= U_3 - U_5 - U_7 - U_{\mathrm{IN2}}, & U_{D3} &= U_4 + U_5 + U_7 + U_{\mathrm{IN2}}, \\ U_{D2} &= -U_4 + U_6 - U_7 - U_{\mathrm{IN2}}, & U_{D4} &= -U_3 - U_6 + U_7 + U_{\mathrm{IN2}}. \end{aligned} \tag{2.50}$$

The current-voltage relation of the diodes reads

$$I = d(U) := \gamma(\exp(\delta U) - 1). \tag{2.51}$$

The artificial capacitance C_S causes a parasitic oscillation. Thus we set $C_S = 0$ in our simulations. Consequently, the system (2.49) represents a DAE of index 2. More information concerning the mathematical model of the ringmodulator is given in [13]. We apply the following parameters in our simulations:

$$\begin{aligned} &R_{G1} = 36.3\ \Omega,\ R_{G2} = R_{G3} = 17.3\ \Omega,\ R_J = R_P = 50\ \Omega,\ R_C = 600\ \Omega,\ R = 25\ \mathrm{k}\Omega, \\ &C = 16\ \mathrm{nF},\ C_P = 10\ \mathrm{nF},\ L_H = 4.45\ \mathrm{H},\ L_{S1} = 2\ \mathrm{mH},\ L_{S2} = L_{S3} = 0.5\ \mathrm{mH}, \\ &\gamma = 40.67286402 \cdot 10^{-9}\ \mathrm{A},\ \delta = 17.7493332\mathrm{V}^{-1}. \end{aligned}$$

For the input signals, we choose two harmonic oscillations with different periods

$$U_{\mathrm{IN1}}(t) = 0.5\mathrm{V} \sin\left(\tfrac{2\pi}{T_1} t\right) \quad \text{and} \quad U_{\mathrm{IN2}}(t) = 2\mathrm{V} \sin\left(\tfrac{2\pi}{T_2} t\right), \tag{2.52}$$

where $T_1 > T_2$ holds. The output voltage of the circuit is U_2. Since the ring modulator produces a multiplicative mixture of the input signals, we expect roughly

$$U_2(t) \approx \mathrm{Const.[V]} \cdot \sin\left(\tfrac{2\pi}{T_1} t + \varphi_1\right) \cdot \sin\left(\tfrac{2\pi}{T_2} t + \varphi_2\right). \tag{2.53}$$

Hence a multirate behaviour with two separate time scales is produced. Consequently, we change from the DAE system (2.49) to the corresponding MPDAE system of the form (2.10).

In our numerical simulations, we apply the method of characteristics presented in Sect. 2.2.2. Thereby, the according boundary value problem (2.43),(2.45) is solved via a finite difference method using a scheme of Dahlquist, see [9]. Although Dahlquist's formula is instable for solving initial value problems of ODEs, the discretisation of boundary value problems succeeds. Furthermore, we use linear interpolation for evaluating the boundary conditions. We fix the slow rate to $T_1 = 1000$ ms, whereas four different cases with respect to the fast rate T_2 are simulated. Fig. 4 illustrates the resulting MVFs for the output voltage. The multidimensional model allows a graphic comparison of the signal's behaviour in time domain. Further numerical simulations using the MPDAE model for a ring modulator circuit are given in [2, 3, 17].

Finally, we use the solution of the MPDAE to reconstruct the corresponding DAE solution via (2.7) in the case $T_1 = 1000$ ms and $T_2 = 0.1$ ms. Consequently, the MVFs allow to reconstruct ten thousand oscillations during one slow period. For comparison, an initial value problem of the DAE (2.49) is solved applying the RADAU5 integrator, see [10], where the solution of the MPDAE in $t_1 = t_2 = 0$ yields the starting values. Fig. 5 demonstrates the results for two different time intervals. We observe a good agreement of both approximations. In particular, the amplitude modulation is resolved correctly.

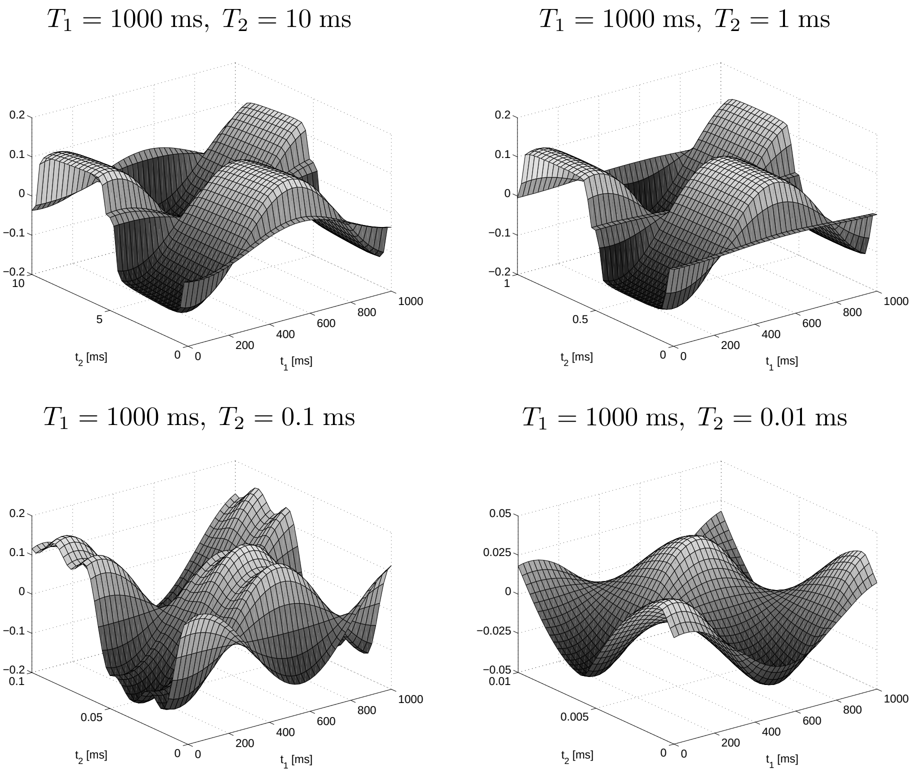

FIGURE 4. MPDAE solutions for $\hat{U}_2$ using different time scales.

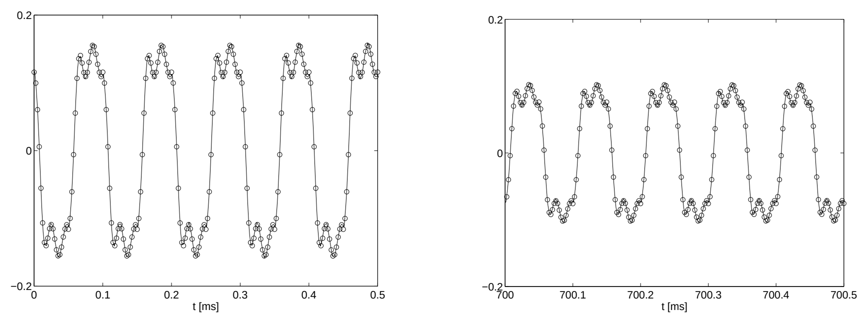

FIGURE 5. Output voltage U_2 obtained by transient analysis of the DAE (solid line) and by reconstruction using the MVF (circles) in time intervals [0 ms, 0.5 ms] and [700 ms, 700.5 ms].

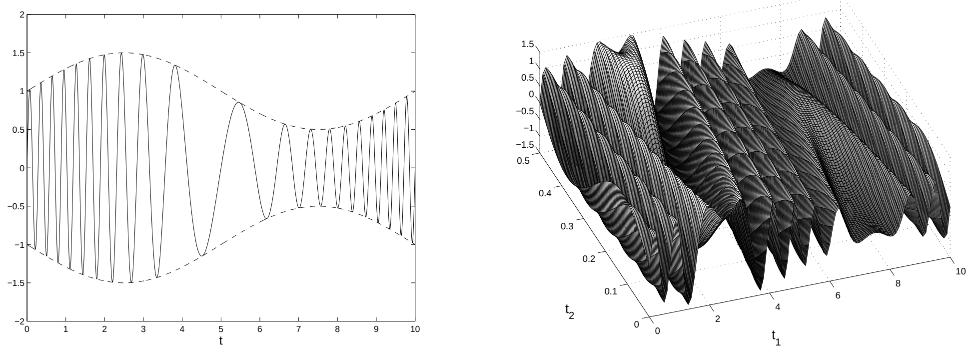

FIGURE 6. Frequency modulated signal x (left) and corresponding naive MVF $\hat{x}$ (right).

3 Model for Frequency Modulation

Now we assume the existence of autonomous parts in an RF circuit, which enable the generation of frequency modulation. Thus we have to modify the signal model as well as the corresponding MPDAE system to tackle this problem efficiently. Although the succession of the survey is analogue to the previous chapter, the analytical and numerical properties of the multivariate model become more sophisticated.

3.1 Multidimensional Approach

3.1.1 *Multivariate Model for AM/FM Signals*

In this section, we consider the presence of frequency modulation in addition to amplitude modulation. For example, the multitone signal

$$x(t) := \left[1 + \alpha \sin\left(\tfrac{2\pi}{T_1} t\right)\right] \cdot \sin\left(\tfrac{2\pi}{T_2} t + \beta \sin\left(\tfrac{2\pi}{T_1} t\right)\right) \tag{3.1}$$

with $T_1 \gg T_2$ includes amplitude modulation introduced by the parameter $0 < \alpha < 1$, whereas the parameter $\beta > 0$ determines the amount of frequency modulation. Fig. 6 (left) illustrates signal (3.1) qualitatively. We can directly specify a corresponding biperiodic MVF via

$$\hat{x}(t_1, t_2) := \left[1 + \alpha \sin\left(\tfrac{2\pi}{T_1} t_1\right)\right] \cdot \sin\left(\tfrac{2\pi}{T_2} t_2 + \beta \sin\left(\tfrac{2\pi}{T_1} t_1\right)\right). \tag{3.2}$$

Again the reconstruction reads $x(t) = \hat{x}(t, t)$. Unfortunately, this MVF includes many oscillations in the according rectangle $[0, T_1] \times [0, T_2]$, see Fig. 6 (right). The number of oscillations increases the larger the parameter β becomes. Thus the naive representation (3.2) is inefficient in the case of frequency modulated signals, although it is suitable for purely amplitude modulated signals.

To obtain an appropriate formulation, Narayan and Roychowdhury [19] propose to model the frequency modulation separately. Accordingly, the MVF just includes the amplitude modulation part, which yields the biperiodic description

$$\hat{y}(t_1, t_2) := \left[1 + \alpha \sin\left(\tfrac{2\pi}{T_1} t_1\right)\right] \cdot \sin\left(2\pi t_2\right), \tag{3.3}$$

where the second period is transformed to 1. The alternative MVF (3.3) exhibits the same form as the MVF (2.4) shown in Fig. 1 (right). Thus we have achieved a simple and efficient representation again. The frequency modulation part is specified by the additional time-dependent function

$$\Psi(t) := \frac{t}{T_2} + \frac{\beta}{2\pi} \sin\left(\tfrac{2\pi}{T_1} t\right). \tag{3.4}$$

We perform the reconstruction of the original signal (3.1) using

$$x(t) = \hat{y}(t, \Psi(t)). \tag{3.5}$$

Thereby, the function (3.4) stretches the second time scale and thus it is called a *warping function*. The derivative of the warping function can be seen as a *local frequency* of the respective signal. In our example, the local frequency results in

$$\nu(t) := \Psi'(t) = \frac{1}{T_2} + \frac{\beta}{T_1} \cos\left(\tfrac{2\pi}{T_1} t\right), \tag{3.6}$$

which represents a simple T_1-periodic function in time. Hence we obtain an efficient multidimensional model for frequency modulated signals by means of a MVF and a corresponding local frequency function. Note that the multivariate representation is not unique here, since a family of MVFs and respective local frequencies can reproduce the same signal.

The outlined multidimensional model can be generalised to an arbitrary finite number of time scales. As we have seen in the above example, the signal (3.1) can be described by the MVF (3.2) with constant frequency as well as by the MVF (3.3) including a varying frequency function. Hence we have the choice to arrange a time scale either with a constant frequency or with varying frequency in the multivariate representation. The suitable way of modelling follows from the structure of the underlying signal.

3.1.2 *Warped MPDAE Model*

If the solution of the DAE (1.1) exhibits frequency modulation, then the multivariate representation implies an MPDAE again. Narayan and Roychowdhury [19] introduced a corresponding system of *warped multirate partial differential algebraic equations*. In the general case of m separate time scales, the system reads

$$\sum_{l=1}^{m} \nu_l(t_1, \ldots, t_m) \frac{\partial \mathbf{q}(\hat{\mathbf{x}})}{\partial t_l} = \mathbf{f}\left(\hat{\mathbf{b}}(t_1, \ldots, t_m), \hat{\mathbf{x}}(t_1, \ldots, t_m)\right), \tag{3.7}$$

where $\nu_l : \mathbb{R}^m \to \mathbb{R}$ represent local frequency functions for $l = 1, \ldots, m$. Setting $\nu_l \equiv c_l$ with a constant $c_l \in \mathbb{R}$ means that the lth time scale is assumed to own a constant frequency or an aperiodic behaviour. If the local frequency is not constant, then an appropriate function is often unknown a priori. Hence the system (3.7) is underdetermined and we need additional conditions to identify adequate local frequencies. Some choices will be discussed in Sect. 3.1.5.

In many applications, the input does not include frequency modulated signals but produces frequency modulation in the output signals. Thus if the MVF $\hat{\mathbf{b}}$ involves (without loss of generality) just the first p variables $t_1, \ldots, t_p$ with $p < m$, then the local frequency functions depend on the same variables only.

In the general case (3.7), there exists no explicit formula for the reconstruction of a corresponding DAE solution. The strategy of reconstruction requires the solution of a system of ordinary differential equations (ODEs) now, which is analysed in Sect. 3.1.3.

To solve the system (3.7), initial and boundary conditions have to be specified. The multidimensional approach is only efficient if all fast time scales exhibit a periodic behaviour. Just the slowest time scale may be periodic or aperiodic.

In electric circuits involving frequency modulation, the common case consists in a forced slow time scale together with an autonomous fast time scale. Thus the input signals operate just at the slow time scale and do not require a multivariate description. Consequently, The corresponding system of warped MPDAEs results to

$$\frac{\partial \mathbf{q}(\hat{\mathbf{x}})}{\partial t_1} + \nu(t_1)\frac{\partial \mathbf{q}(\hat{\mathbf{x}})}{\partial t_2} = \mathbf{f}(\mathbf{b}(t_1), \hat{\mathbf{x}}(t_1, t_2)). \tag{3.8}$$

Since we assume that the input produces the frequency modulation, the local frequency function depends on the same variable as the input. In this specific case, it is straightforward to reconstruct a solution of the DAE (1.1) via

$$\mathbf{x}(t) := \hat{\mathbf{x}}\left(t, \int_0^t \nu(s)\,\mathrm{d}s\right), \tag{3.9}$$

which accords to the signal model outlined in Sect. 3.1.1.

The resulting boundary conditions for the warped MPDAE (3.8) are analogue to the case of constant frequencies, cf. Sect. 2.1.2. If the input signal is aperiodic, then we obtain an initial-boundary value problem (2.12) with $T_2 = 1$. The second period is standardised to 1, whereas the local frequency specifies the magnitude of the second time scale. In case of T_1-periodic input signals, the pure boundary value problem (2.11) with $T_2 = 1$ arises, where a biperiodic solution shall be determined. Furthermore, the discussion from Sect. 2.1.4 can be performed in an analogue way to verify the well-posedness of the system (3.8).

3.1.3 *Characteristic System of the Warped MPDAE*

According to the multirate system (2.6), warped MPDAE systems exhibit a hyperbolic structure, too. Thus we obtain a corresponding *characteristic system*, which describes the transport of information completely. The characteristic system of the general warped MPDAE (3.7) reads

$$\begin{aligned} \tfrac{\mathrm{d}}{\mathrm{d}\tau} t_l(\tau) &= \nu_l(t_1(\tau), \ldots, t_m(\tau)), \quad l = 1, \ldots, m \\ \tfrac{\mathrm{d}}{\mathrm{d}\tau} \mathbf{q}(\hat{\mathbf{x}}(\tau)) &= \mathbf{f}\left(\mathbf{b}(t_1(\tau), \ldots, t_m(\tau)), \hat{\mathbf{x}}(\tau)\right), \end{aligned} \tag{3.10}$$

where the variables t_l as well as the MVF $\hat{\mathbf{x}}$ depend on a parameter τ again. For given local frequency functions, the part for the variables $t_1, \ldots, t_m$ represents a system of ODEs. A solution of this system yields the *characteristic projections*. If solutions of corresponding initial value problems are always unique, then two different characteristic projections never intersect. For example, the uniqueness can be guaranteed via $\nu_l \in C^1$ for all l.

In contrast to constant frequencies, we do not have an explicit formula for the characteristic projections in this general case. Considering a specific characteristic projection, we obtain the whole *characteristic curve* by solving the last equation in (3.10), which represents a system of DAEs. The solution of (3.10) with initial values

$$t_1(0) = \cdots = t_m(0) = 0, \quad \hat{\mathbf{x}}(0) = \mathbf{x}_0 \tag{3.11}$$

recovers a solution of the original DAE (1.1). Therefore solving the ODE part in (3.10) is necessary to obtain the reconstruction scheme for solutions of the underlying DAE.

In the important case (3.8) with two time scales, we obtain the characteristic system

$$\begin{aligned} \tfrac{\mathrm{d}}{\mathrm{d}\tau} t_1(\tau) &= 1 \\ \tfrac{\mathrm{d}}{\mathrm{d}\tau} t_2(\tau) &= \nu(t_1(\tau)) \\ \tfrac{\mathrm{d}}{\mathrm{d}\tau} \mathbf{q}(\hat{\mathbf{x}}(\tau)) &= \mathbf{f}\left(\mathbf{b}(t_1(\tau)), \hat{\mathbf{x}}(\tau)\right). \end{aligned} \tag{3.12}$$

Hence we are able to solve the part for the variables t_1, t_2 explicitly and thus we obtain characteristic projections of the form

$$t_2(t_1) = \int_0^{t_1} \nu(s)\ \mathrm{d}s + c \qquad \text{for arbitrary } \ c \in \mathbb{R}, \tag{3.13}$$

which generate a continuum of parallel curves in the domain of dependence.

3.1.4 *Transformation Properties*

We can transform a MVF satisfying the general system (3.7) for a specific local frequency function into a MVF fulfilling the system with another local frequency. However, such a transformation is only interesting, if it does not change a certain initial manifold. In case of two time scales, a MVF $\hat{\mathbf{x}}$ solving the MPDAE (3.8) for a local frequency function $\nu \in C^0$ can be transformed to another MVF $\hat{\mathbf{y}}$ satisfying the system with an arbitrary local frequency $\mu \in C^0$ via

$$\hat{\mathbf{y}}(t_1, t_2) := \hat{\mathbf{x}}\left(t_1, t_2 + \int_0^{t_1} \nu(s) - \mu(s)\ \mathrm{d}s\right). \tag{3.14}$$

The initial manifold $\{(t_1, t_2) \in \mathbb{R}^2 : t_1 = 0\}$ is invariant in this transformation. In particular, both solutions yield the same solution of the underlying DAE (1.1) in the corresponding reconstructions (3.9), since it holds

$$\mathbf{x}(t) := \hat{\mathbf{x}}\left(t, \int_0^t \nu(s)\ \mathrm{d}s\right) = \hat{\mathbf{y}}\left(t, \int_0^t \mu(s)\ \mathrm{d}s\right). \tag{3.15}$$

Hence the local frequencies represent free parameters in the multidimensional approach, which we can specify to achieve an efficient representation by corresponding MVFs. However, we do not have knowledge about the solutions a priori. Thus we need additional conditions, which identify appropriate local frequency functions.

For biperiodic MVFs, the involved local frequency functions have to satisfy some restrictions in order to preserve the periodicities in the transformation (3.14). The four properties

$$\begin{array}{llll} \text{(i)} & \hat{\mathbf{x}} \in C^1 \ \text{ is } (T_1, 1)\text{-periodic,} & \text{(iii)} & \mu \in C^0 \ \text{ is } T_1\text{-periodic,} \\ \text{(ii)} & \nu \in C^0 \ \text{ is } T_1\text{-periodic,} & \text{(iv)} & \int_0^{T_1} \mu(s)\ \mathrm{d}s = \int_0^{T_1} \nu(s)\ \mathrm{d}s \end{array} \tag{3.16}$$

guarantee that the function $\hat{\mathbf{y}} \in C^1$ defined by (3.14) is $(T_1, 1)$-periodic, too. The requirements (i)-(iii) are obvious. Defining the average frequency of a periodic local frequency function $\sigma \in C^0$ as

$$\overline{\sigma} := \frac{1}{T_1} \int_0^{T_1} \sigma(s) \, \mathrm{d}s, \tag{3.17}$$

property (iv) implies that the average frequencies coincide, i.e. $\overline{\nu} = \overline{\mu}$. Therefore the existence of one biperiodic solution yields a family of solutions with same average frequency generated via (3.14). In particular, a solution corresponding to constant local frequency $\overline{\nu}$ exists, i.e. it satisfies a standardised form of the MPDAE (2.10).

Furthermore, the specific system (3.8) is autonomous in the second time scale. Thus, given a MVF satisfying the system, the shifted function

$$\hat{\mathbf{z}}(t_1, t_2) := \hat{\mathbf{x}}(t_1, t_2 + c) \quad \text{for constant } \ c \in \mathbb{R} \tag{3.18}$$

represents a solution corresponding to the same local frequency function again. This transformation, which is obvious on the MPDAE level, represents a hidden degree of freedom in solutions of the original DAE system (1.1).

3.1.5 *Additional Conditions*

In this section, we discuss the identification of adequate local frequency functions. We restrict to the case of two time scales described by the system (3.8), where just one frequency function has to be specified. If widely separated time scales arise, then small changes in the local frequency function cause huge deformations in the corresponding MVFs due to the transformation (3.14), see [24]. In view of this sensitivity, we can not expect that an a priori specification of the local frequencies yields a suitable solution. Thus the local frequency function has to be determined indirectly by additional conditions, which use the representation by MVFs.

Narayan and Roychowdhury [19] propose a continuum of *phase conditions*, which control the phase in each cross section of the MVF corresponding to a constant value t_1. Without loss of generality, we choose the first component of the MVF $\hat{\mathbf{x}} = (\hat{x}^1, \ldots, \hat{x}^k)^\top$. In time domain, an example for a phase condition reads

$$\hat{x}^1(t_1, 0) = \eta(t_1) \quad \text{for all } \ t_1 \in \mathbb{R} \tag{3.19}$$

with predetermined function $\eta : \mathbb{R} \to \mathbb{R}$. Appropriate constant choices $\eta \equiv \eta_0$ are often sufficient. Another example is given by

$$\frac{\partial \hat{x}^1}{\partial t_2}(t_1, 0) = \eta(t_1) \quad \text{for all } \ t_1 \in \mathbb{R}. \tag{3.20}$$

Thereby, the demand $\eta \equiv 0$ is often suitable. The constant choices represent multidimensional generalisations of phase conditions for DAEs. Both (3.19) and (3.20) yield an additional boundary condition in time domain. The existence of corresponding solutions can be motivated by the implicit function theorem and employing the transformations (3.14) and (3.18). We may apply these phase conditions for solving pure boundary value problems (2.11) as well as initial-boundary value problems (2.12).

If the fast time scale is transformed in frequency domain, then phase conditions can be based on Fourier coefficients of the MVF, see [19]. A simple example is the demand

$$\mathrm{Im}(X_j^1(t_1)) = 0 \quad \text{for all } \ t_1 \in \mathbb{R}, \tag{3.21}$$

where $\mathrm{Im}(X_j^1) : \mathbb{R} \to \mathbb{R}$ represents the imaginary part of the jth coefficient in the Fourier expansion applied to the first component $\hat{x}^1$. Zhu and Christoffersen [35, 36] succeed in using conditions with Fourier coefficients for numerical simulations.

In general, elementary phase conditions already yield simple and thus efficient solutions of the MPDAE system. However, this favourable property can not be proved universally. Therefore another idea consists in demanding some condition, which incorporates the complete MVF and thus enables the determination of an optimal solution in some sense.

Houben [11] introduces a *minimisation criterion* of the form

$$\beta(t_1) := \int_0^1 \left\| \frac{\partial \mathbf{q}(\hat{\mathbf{x}})}{\partial t_1} \right\|^2 \mathrm{d}t_2 \quad \to \quad \text{min.} \qquad \text{for each } \ t_1 \tag{3.22}$$

using the Euclidean norm $\| \cdot \|$. The arising function β includes just the derivative with respect to the slow time scale, since the derivative corresponding to the fast time scale is invariant in the transformation (3.14). The example in Sect. 3.1.1 illustrates that inappropriate MVFs exhibit many oscillations in the direction of the slow time scale. Now this disadvantageous behaviour is decreased by using the demand (3.22).

An according calculus yields an explicit formula for the optimal local frequencies depending on the MVF, namely

$$\nu_{\text{opt}}(t_1) = \frac{\displaystyle\int_0^1 \left\langle \mathbf{f}\left(\mathbf{b}(t_1), \hat{\mathbf{x}}(t_1, t_2)\right), \tfrac{\partial \mathbf{q}(\hat{\mathbf{x}})}{\partial t_2} \right\rangle \mathrm{d}t_2}{\displaystyle\int_0^1 \left\| \tfrac{\partial \mathbf{q}(\hat{\mathbf{x}})}{\partial t_2} \right\|^2 \mathrm{d}t_2} \tag{3.23}$$

applying the Euclidean scalar product $< \cdot, \cdot >$. Inserting (3.23) in the MPDAE (3.8) allows to solve initial-boundary value problems (2.12) directly. However, instead of using the solution $\hat{\mathbf{x}}$ itself, the minimisation is based on the function $\mathbf{q}(\hat{\mathbf{x}})$ in order to replace corresponding derivatives by terms in (3.8). In many cases, the MVF $\hat{\mathbf{x}}$ will be efficient if and only if $\mathbf{q}(\hat{\mathbf{x}})$ represents a simple function. Yet this property can not be guaranteed in general. Moreover, considering a semi-explicit DAE for (1.1), the minimisation does not involve the algebraic variables.

Thus another approach consists in minimising the derivatives of the MVF itself, see [27]. Considering biperiodic boundary value problems (2.11), the corresponding demand reads

$$\gamma\left(\hat{\mathbf{x}}\right) := T_1 \int_0^{T_1} \int_0^1 \sum_{l=1}^{k} w_l \left(\frac{\partial \hat{x}^l}{\partial t_1} \right)^2 \mathrm{d}t_2 \; \mathrm{d}t_1 \quad \to \quad \text{min.} \tag{3.24}$$

with constant weights $w_1, \ldots, w_k \geq 0$. The weights can be used to perform an appropriate scaling in each component, if the corresponding physical quantities differ by several orders of magnitude. Moreover, setting some weights to zero allows to focus on an arbitrary subset of components.

Based on the transformation formula (3.14), a corresponding *variational calculus* implies a necessary condition for an optimal solution, namely

$$r(t_1) := \int_0^1 \sum_{l=1}^{k} w_l \cdot \frac{\partial^2 \hat{x}^l}{\partial {t_1}^2} \cdot \frac{\partial \hat{x}^l}{\partial t_2} \, \mathrm{d}t_2 = 0 \quad \text{for all } \ t_1 \in \mathbb{R}. \tag{3.25}$$

In contrast to the phase conditions (3.19) and (3.20), the requirement (3.25) is not a boundary condition, but depends on values in the complete biperiodic domain of dependence, which is needed to perform the minimisation everywhere. If an arbitrary biperiodic solution of the MPDAE (3.8) exists, then the existence of an optimal function with respect to the minimisation (3.24) can be expected in the continuum of transformed solutions. In case of initial-boundary value problems (2.12), alternative minimisation criteria imposed on the MVF itself have to be considered.

All presented conditions involve scalar functions depending on the slow time scale. Thus the structure of an additional demand always agrees to the amount of free parameters in the problem, since the local frequency function represents a scalar function depending on the slow time scale, too.

Furthermore, the existence of a biperiodic solution implies a continuum of biperiodic solutions with same local frequency function via the translation (3.18). Thus for biperiodic boundary value problems (2.11), another extra condition is necessary to isolate a specific solution from the continuum. For this purpose, we may apply scalar phase conditions like

$$\hat{x}^1(0,0) = \eta_0 \qquad \text{or} \qquad \frac{\partial \hat{x}^1}{\partial t_2}(0,0) = \eta_0 \qquad \text{for a constant } \ \eta_0 \in \mathbb{R}. \tag{3.26}$$

In the first variant, the constant η_0 has just to be chosen out of the range of $\hat{x}^1(0,\cdot)$. In the second type, the choice $\eta_0 = 0$ is always feasible, since $\hat{x}^1(0,\cdot)$ is a smooth and periodic function. Employing the continuous phase condition (3.19) or (3.20), this specification is done automatically.

3.2 Numerical Methods

In general, we can modify a numerical technique for solving the MPDAE (2.6) into a method for solving the warped MPDAE (3.7). We outline these transitions for the methods presented in Sect. 2.2. Thereby, we consider the system (3.8) with two time scales. Consequently, an additional condition to identify the local frequency function, see Sect. 3.1.5, has to be included in each scheme.

3.2.1 *Frequency Domain Methods*

In this section, we sketch the construction of a pure frequency domain method to solve the biperiodic boundary value problem (2.11) of the MPDAE (3.8). Following Sect. 2.2.1, we apply the finite sum (2.26) with $\omega_2 = 2\pi$ as approximation for the $(T_1, 1)$-periodic MVF. Again the partial derivatives in the MPDAE are given by a modification of the according coefficients, see (2.27). However, the partial derivative with respect to t_2 is multiplied with the local frequency in the MPDAE. Thus we obtain additional coefficients for the biperiodic function

$$\nu(t_1)\frac{\partial \mathbf{q}(\hat{\mathbf{x}})}{\partial t_2}(t_1,t_2) \doteq \sum_{j_1=-p_1}^{p_1}\sum_{j_2=-p_2}^{p_2} \hat{\mathbf{R}}_{j_1,j_2}(\hat{\mathbf{X}},\nu)\exp\left(i(\omega_1 j_1 t_1 + 2\pi j_2 t_2)\right). \tag{3.27}$$

These values depend on the coefficients $\hat{\mathbf{X}}_{j_1,j_2}$ as well as on the local frequency function, which represents a drawback in frequency domain methods applied to warped MPDAEs in comparison to common MPDAEs. The corresponding Galerkin approach yields the nonlinear system

$$\hat{\mathbf{G}}_{j_1,j_2}(\hat{\mathbf{X}}) := i\omega_1 j_1 \hat{\mathbf{Q}}_{j_1,j_2}(\hat{\mathbf{X}}) + \hat{\mathbf{R}}_{j_1,j_2}(\hat{\mathbf{X}},\nu) - \hat{\mathbf{F}}_{j_1,j_2}(\hat{\mathbf{X}}) = \mathbf{0} \tag{3.28}$$

for $j_1 = -p_1,\ldots,p_1,\ j_2 = -p_2,\ldots,p_2$. Nevertheless, since the values $\hat{\mathbf{Q}}_{j_1,j_2}(\hat{\mathbf{X}})$ have to be computed to handle the first derivative, these coefficients can be used to evaluate the second derivative in time domain. Given some T_1-periodic function ν, the term on the left-hand side in (3.27) can be transformed in frequency domain.

As usual, the periodic local frequency function is unknown a priori. If a representation of the form

$$\nu(t_1) = \sum_{j_1=-\infty}^{\infty} N_{j_1}\exp\left(i\omega_1 j_1 t_1\right) \tag{3.29}$$

exists, then choosing a finite sum yields a tuple of unknown coefficients. Furthermore, we may apply an approximation for ν by defining a set of T_1-periodic functions, which depend on some parameters. The unknown parameters are determined via additional conditions obtained from phase conditions, for example.

According to Sect. 2.2.1, an approach in frequency domain causes a nonlinear system for the involved Fourier coefficients. In corresponding Newton methods, the evaluation of the system and its Jacobian matrix has to be done by appropriate transformations between time and frequency domain. Methods of this type have not been used to simulate practical examples of warped MPDAEs yet.

3.2.2 *Time Domain Methods*

The possibly simplest algorithm to solve biperiodic boundary value problems of the warped MPDAE (3.8) is produced by a discretisation of the partial derivatives using a uniform grid in time domain. This approach corresponds to the finite difference methods presented in Sect. 2.2.2. According to the problem (2.11), we consider the periods T_1 and $T_2 = 1$. For example, if we employ symmetric differences with respect to the grid (2.32) again, then we obtain the nonlinear equations

$$\begin{aligned} &\tfrac{1}{2h_1}\left[\mathbf{q}(\hat{\mathbf{x}}_{j_1+1,j_2}) - \mathbf{q}(\hat{\mathbf{x}}_{j_1-1,j_2})\right] + \nu_{j_1}\tfrac{1}{2h_2}\left[\mathbf{q}(\hat{\mathbf{x}}_{j_1,j_2+1}) - \mathbf{q}(\hat{\mathbf{x}}_{j_1,j_2-1})\right] \\ = \;& \mathbf{f}(\mathbf{b}(t_{1,j_1}),\hat{\mathbf{x}}_{j_1,j_2}) \end{aligned} \tag{3.30}$$

for $j_1 = 1,\ldots,n_1,\ j_2 = 1,\ldots,n_2$. Thereby, the values

$$\nu_{j_1} \doteq \nu(t_{1,j_1}) \quad \text{for } j_1 = 1,\ldots,n_1 \tag{3.31}$$

represent additional unknowns. Thus a system of $n_1 n_2 k$ equations for $n_1 n_2 k + n_1$ unknowns arises. To achieve a well-defined approximation, further conditions have to be included. The phase condition (3.19) yields directly n_1 additional equations. Likewise, n_1 equations can be obtained by discretising the phase condition (3.20) with respect to the uniform grid.

Furthermore, an according approximation of (3.25) on the uniform grid allows to use the condition from the minimisation criterion (3.24). For example, a straightforward discretisation produces the approximation

$$\begin{aligned} r(t_{1,j_1}) \quad &\doteq \quad h_2 \sum_{j_2=1}^{n_2} \sum_{l=1}^{k} w_l \cdot \tfrac{1}{h_1{}^2} \left[\hat{x}^l_{j_1-1,j_2} - 2\hat{x}^l_{j_1,j_2} + \hat{x}^l_{j_1+1,j_2} \right] \\ &\qquad\qquad \cdot \tfrac{1}{2h_2} \left[\hat{x}^l_{j_1,j_2+1} - \hat{x}^l_{j_1,j_2-1} \right] \qquad = \quad 0 \end{aligned} \tag{3.32}$$

for $j_1 = 1, \ldots, n_1$. Applying the periodicities, just values from the grid points are involved here. The computational work of the arising method results not significantly higher in comparison to techniques using phase conditions, since the discretisation of the MPDAE system causes the main effort. Recall that only n_1 conditions are added to a system of $n_1 n_2 k$ equations. Finite difference methods including the additional conditions (3.32) have been successfully used for numerical simulations, see [27].

In Sect. 2.2.2, a method of characteristics has been presented for solving biperiodic problems in case of constant frequencies. This approach can be transfered to the warped MPDAE system, too, using the transport of information outlined in Sect. 3.1.3. However, the construction of the technique becomes more complicated, since the characteristic projections depend on the a priori unknown local frequency. Nevertheless, we obtain an efficient and robust method for solving the biperiodic problem (2.11), see also [24].

We consider widely separated time scales, i.e. $\nu(t_1) \gg T_1^{-1}$ for all t_1, in the following. In particular, it holds $\nu \geq 0$. Like in the previous method of characteristics, we choose the initial points (2.42). According to the characteristic system (3.12), a unique characteristic projection belongs to each initial point given by

$$t_{1,j_1}(\tau) = \tau + (j_1 - 1)h_1, \quad t_{2,j_1}(\tau) = \int_{(j_1-1)h_1}^{(j_1-1)h_1+\tau} \nu(s)\, \mathrm{d}s \quad \text{for } j_1 = 1, \ldots, n_1. \tag{3.33}$$

Fig. 7 illustrates the arising characteristic projections. The last equation in (3.12) yields the corresponding characteristic systems for $\tilde{\mathbf{x}}_{j_1}(\tau) := \hat{\mathbf{x}}(t_{1,j_1}(\tau), t_{2,j_1}(\tau))$

$$\frac{\mathrm{d}\mathbf{q}(\tilde{\mathbf{x}}_{j_1})}{\mathrm{d}\tau}(\tau) = \mathbf{f}\left(\mathbf{b}(\tau + (j_1 - 1)h_1), \tilde{\mathbf{x}}_{j_1}(\tau)\right) \quad \text{for } j_1 = 1, \ldots, n_1. \tag{3.34}$$

The j_1th projection (3.33) intersects the line $t_2 = 1$ in an end point corresponding to the value τ_{j_1}. Since the characteristic projections depend on the frequency function, the n_1 parameters τ_{j_1} are unknown a priori. Again we can use the solution obtained from the DAE systems (3.34) to interpolate the points required for the periodicity condition in the second time scale. Hence the resulting boundary conditions exhibit the form

$$(\tilde{\mathbf{x}}_1(0), \ldots, \tilde{\mathbf{x}}_{n_1}(0))^\top = \mathcal{B}(\tilde{\mathbf{x}}_1(\tau_1), \ldots, \tilde{\mathbf{x}}_{n_1}(\tau_{n_1}))^\top. \tag{3.35}$$

Thereby, the matrix $\mathcal{B} \in \mathbb{R}^{n_1 k \times n_1 k}$ depends on the used interpolation scheme and the unknown parameters $\tau_1, \ldots, \tau_{n_1}$.

The selection of the initial points suggests to use the discretisation (3.31) of the local frequency function again. A quadrature scheme generates an approximation of the

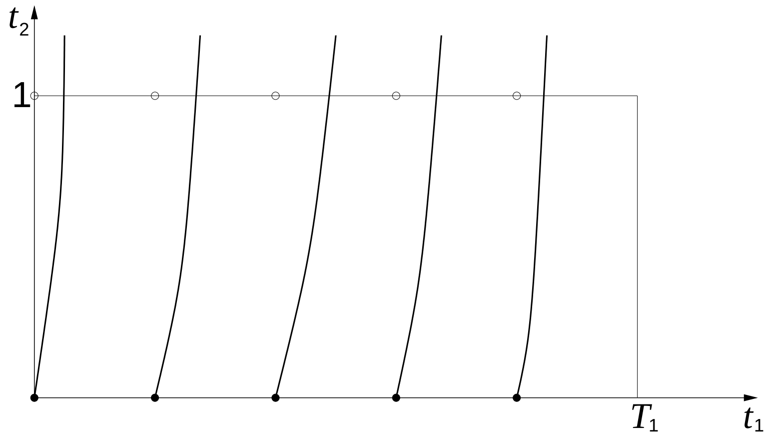

FIGURE 7. Characteristic projections of warped MPDAE in domain of dependence.

integrals in (3.33), where we employ exclusively the values from (3.31). For example, in case of largely differing time scales, trapezoidal rule approximates the j_1th characteristic projection by a quadratic polynomial

$$t_{2,j_1}(\tau) = \int_{(j_1-1)h_1}^{(j_1-1)h_1+\tau} \nu(s)\,\mathrm{d}s \doteq \left(\tau - \frac{\tau^2}{2h_1}\right)\nu_{j_1} + \frac{\tau^2}{2h_1}\nu_{j_1+1} \quad \text{for } \tau \in [0, h_1]. \tag{3.36}$$

If an initial guess for the local frequency is given, we obtain an approximation for the end points $\tau_1, \ldots, \tau_{n_1}$ and thus we can evaluate the nonlinear system (3.35).

The strategy leads to a boundary value problem of DAEs given by (3.34),(3.35). We can solve the problem numerically using shooting methods or finite difference methods, for example. Phase conditions are able to specify the additional unknowns (3.31). The requirement (3.19) can be added directly to the boundary conditions (3.35), since only initial values are involved. On the other hand, an appropriate discretisation of the demand (3.20) is necessary for achieving a condition, which depends just on the initial values. Both phase conditions have been successfully used in methods of characteristics, see [25].

The inclusion of requirements from minimisation criteria like (3.32), for example, becomes more difficult, since values of the solution outside the characteristic systems are needed. Nevertheless, if we apply a finite difference method for solving (3.34),(3.35), quantities from a characteristic grid can be interpolated on a uniform grid just to evaluate the conditions (3.32). Thus the use of methods of characteristics involving conditions for optimal solutions is feasible.

For solving initial-boundary value problems (2.12) in time domain, the construction of techniques based on semidiscretisation is obvious, cf. Sect. 2.2.2. Houben [11] employs a method of lines to solve the MPDAE (3.8), where the local frequency function is replaced by (3.23). Using phase conditions, the approximative DAE systems from the semidiscretisation have to include additional conditions or have to be modified appropriately. Theory and numerical behaviour of such techniques are topics of current research. The application of some elementary schemes is investigated in [26].

3.2.3 *Mixed Domain Techniques*

We discuss briefly the use of mixed time-frequency domain methods for warped MPDAEs. The motivation of these methods is the same as explained in Sect. 2.2.3. Corresponding techniques are introduced in [19]. The MVF is approximated by the finite sum (2.46) with $\omega_2 = 2\pi$. Consequently, the MPDAE (3.8) yields the condition

$$\sum_{j_2=-p_2}^{p_2} \left[\frac{\mathrm{d}\hat{\mathbf{Q}}_{j_2}(\hat{\mathbf{X}})}{\mathrm{d}t_1}(t_1) + i2\pi j_2 \nu(t_1)(\hat{\mathbf{Q}}_{j_2}(\hat{\mathbf{X}}))(t_1) - (\hat{\mathbf{F}}_{j_2}(\hat{\mathbf{X}}))(t_1) \right] \cdot \exp(i2\pi j_2 t_2) = \mathbf{0}, \tag{3.37}$$

where $(\hat{\mathbf{Q}}_{j_2}(\hat{\mathbf{X}}))(t_1)$ and $(\hat{\mathbf{F}}_{j_2}(\hat{\mathbf{X}}))(t_1)$ denote the Fourier coefficients of the functions $\mathbf{q}(\hat{\mathbf{x}}(t_1,\cdot))$ and $\mathbf{f}(\mathbf{b}(t_1), \hat{\mathbf{x}}(t_1,\cdot))$, respectively. Since the basis functions are orthogonal, we obtain the coupled systems

$$\frac{\mathrm{d}\hat{\mathbf{Q}}_{j_2}(\hat{\mathbf{X}})}{\mathrm{d}t_1}(t_1) = (\hat{\mathbf{F}}_{j_2}(\hat{\mathbf{X}}))(t_1) - i2\pi j_2 \nu(t_1)(\hat{\mathbf{Q}}_{j_2}(\hat{\mathbf{X}}))(t_1), \quad j_2 = -p_2, \ldots, p_2. \tag{3.38}$$

Hence a system of DAEs for the unknown functions in the approximation (2.46) results. Initial or boundary value problems of this system arise as demonstrated in Sect. 2.2.3.

However, the local frequency function ν is unknown. We achieve a well-defined DAE system by demanding a condition, which involves the Fourier coefficients. For example, requirements like (3.21) directly prescribe the real or imaginary part of an unknown function. Numerical simulations employing conditions with Fourier coefficients are presented in [35, 36]. Moreover, phase conditions defined in time domain can be transformed into frequency domain to get equivalent requirements, which possibly couple all functions.

3.3 Illustrative Example: Colpitt Oscillator

To simulate a realistic electric circuit again, we examine a forced Colpitt oscillator. The Colpitt oscillator represents a typical LC-oscillator. The circuit includes one inductance, four capacitances and a bipolar transistor, see Fig. 8. A specific mathematical model of the Colpitt oscillator leads to an implicit ODE system, which describes the transient behaviour of four node voltages, namely

$$\begin{pmatrix} 1 & 0 & 0 & 0 \\ 0 & C_1 + C_3 & -C_3 & -C_1 \\ 0 & -C_3 & C_2 + C_3 + C_4 & -C_2 \\ 0 & -C_1 & -C_2 & C_1 + C_2 \end{pmatrix} \begin{pmatrix} \dot{U}_1 \\ \dot{U}_2 \\ \dot{U}_3 \\ \dot{U}_4 \end{pmatrix} =$$

$$\begin{pmatrix} \frac{R_2}{L}(U_2 - U_1) + R_2 \dot{U}_{op} \\ \frac{1}{R_2}(U_{op} - U_1) + \left(I_S + \frac{I_S}{b_C}\right) g(U_4 - U_2) - I_S g(U_4 - U_3) \\ -\frac{1}{R_4}U_3 + \left(I_S + \frac{I_S}{b_E}\right) g(U_4 - U_3) - I_S g(U_4 - U_2) \\ -\frac{1}{R_3}U_4 + \frac{1}{R_1}(U_{op} - U_4) - \frac{I_S}{b_E} g(U_4 - U_3) - \frac{I_S}{b_C} g(U_4 - U_2) \end{pmatrix}. \tag{3.39}$$

The applied transistor model includes the nonlinear function

$$g(U) = \exp\left(\frac{U}{U_T}\right) - 1. \tag{3.40}$$

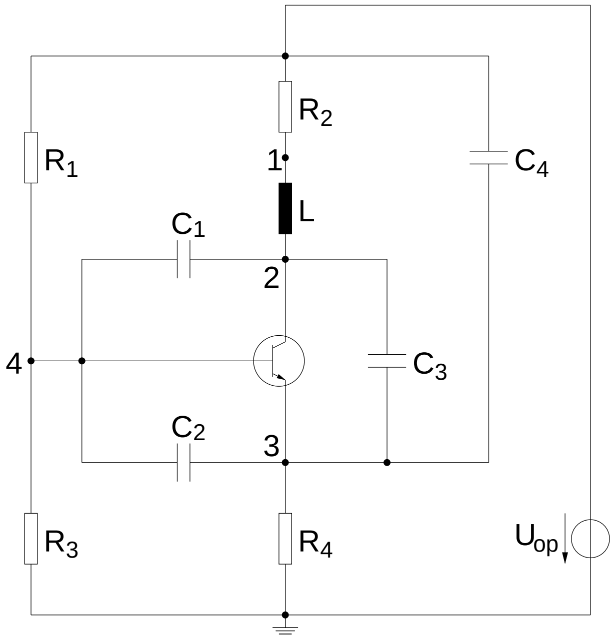

Figure 8. Circuit of Colpitt oscillator.

The technical parameters are set to the values

$$
\begin{aligned}
&C_1 = 50 \text{ pF},\ C_2 = 1 \text{ nF},\ C_3 = 50 \text{ nF},\ C_4 = 100 \text{ nF},\ R_1 = 12 \text{ k}\Omega,\\
&R_2 = 3\ \Omega,\ R_3 = 8.2 \text{ k}\Omega,\ R_4 = 1.5 \text{ k}\Omega,\ L = 10 \text{ mH},\ U_{op} = 10 \text{ V},\\
&I_S = 1 \text{ mA},\ b_E = 100,\ b_C = 50,\ U_T = 25.85 \text{ mV}.
\end{aligned}
$$

Using these parameters, the Colpitt oscillator owns a periodic solution with time rate $T_0 = 0.125$ ms. More details about the modelling of the Colpitt oscillator can be found in [13].

Now an external source controls the third capacitor

$$C_3(t) = 50 \text{ nF} \left(1 + 0.8 \sin\left(\tfrac{2\pi}{T_1} t\right)\right) \tag{3.41}$$

and we choose $T_1 = 1$ s, see Fig. 9 (left). Hence the capacitance matrix in (3.39) becomes time-dependent and the system is no longer of the form (1.1). Nevertheless, the resulting capacitance matrix is always regular. Thus the arising system is equivalent to an explicit ODE, which represents a special case of (1.1).

The time-dependent capacitance (3.41) introduces frequency modulation at widely separated time scales. Thus we apply the warped MPDE model corresponding to the ODE (3.39). The phase condition (3.20) with $\eta \equiv 0$ is added to determine the local frequency function. To solve the biperiodic boundary value problem (2.11), we use the method of characteristics from Sect. 3.2.2. A shooting method solves the arising boundary value problem (3.34),(3.35) of ODEs approximately, where trapezoidal rule is applied in the numerical integrations. More information concerning this simulation can be found in [24].

Fig. 9 (right) illustrates the arising local frequency function. Where the capacitance

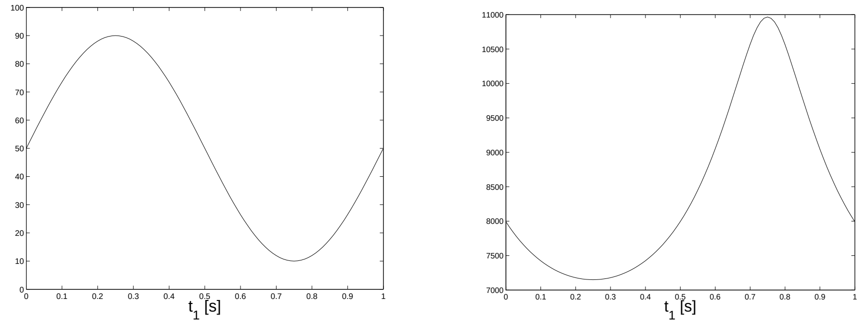

FIGURE 9. Input signal C_3[nF] (left) and resulting local frequency $\nu[\mathrm{s}^{-1}]$ (right).

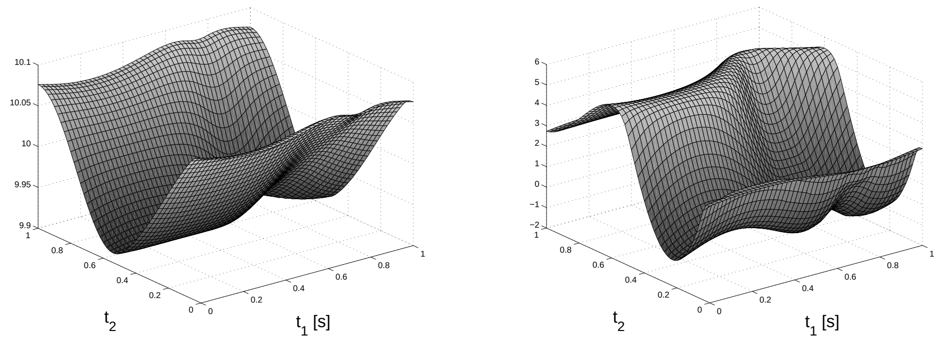

FIGURE 10. MVFs $\hat{U}_1$[V] (left) and $\hat{U}_4$[V] (right).

is low, the frequency is high in a nonlinear relation. This behaviour is typical for LC-oscillators. Thus the phase condition is able to determine physically reasonable frequencies. The MVFs for U_1 and U_4 are shown in Fig. 10. Each function exhibits just one oscillation in each coordinate direction, and thus an efficient representation is achieved. Furthermore, we see the performance of the phase condition (3.20) in the first component.

Finally, we also reconstruct the corresponding quasiperiodic solution of (3.39) using the relation (3.9). For comparison, an initial value problem of (3.39) is solved by trapezoidal rule, where the MPDE solution yields the starting values. Fig. 11 demonstrates the resulting signals for the most interesting component U_4. In the first few cycles, we observe a good agreement between both approximations. In later cycles, a phase shift occurs due to two reasons. Firstly, small numerical errors in the local frequency function are amplified during many oscillations. Secondly, the transient integration causes a phase shift in comparison to the exact solution, too, which represents a more general problem. Nevertheless, the other signal properties agree also in later cycles, i.e. the amplitude, the shape and the frequency.

4 Conclusions and Outlook

The simulation of radio frequency circuits is quite time consuming, if based on differential algebraic models commonly used in circuit simulation packages to describe its transient

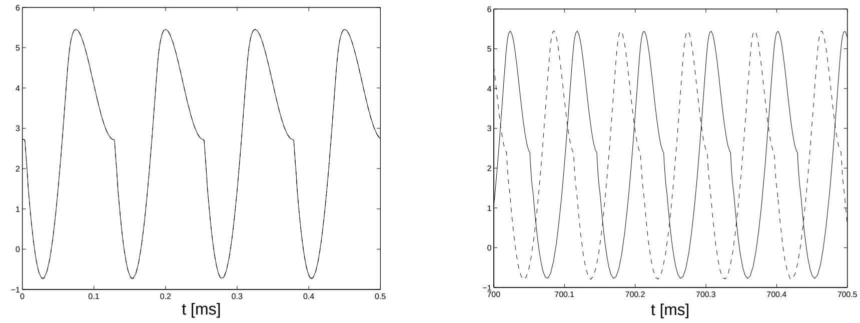

FIGURE 11. ODE solution U_4[V] integrated (solid line) and interpolated from MVFs (dashed line) in time intervals [0ms, 0.5ms] (left) and [700ms, 700.5ms] (right).

behaviour: here the fast rate restricts the step size in time. This problem can be overcome by replacing multitone signals via multivariate functions and, correspondingly, by transforming the DAE model into a singular PDE model. This transition decouples the widely separated time scales of RF signals and allows for a reconstruction of the original time-dependent signal. The arising modelling approach can be generalised from systems with only amplitude modulation to systems with amplitude and/or frequency modulation. For both MPDAE models, the original and the warped version, different numerical techniques proposed so far in the literature have shown their practicability in numerical simulations of RF circuits.

Two main tasks remain for the future: on the one hand, it has to be checked whether modelling via MPDAEs can be applied in an efficient way to other areas of application besides RF circuits. For example, flexible multibody systems might be a promising starting point. On the other hand, appropriate strategies for partitioning a circuit by introducing appropriate couplings are desirable, which allow to apply the MPDAE model to several subcircuits separately. In a complex circuit, the individual parts possibly exhibit different multirate behaviour. Thus each subcircuit may demand its own MPDAE system or an alternative technique in case of completely aperiodic time scales.

Acknowledgements

This work is part of the BMBF programme “Multiskalensysteme in Mikro- und Optoelektronik” within the project “Partielle Differential-Algebraische Multiskalensysteme für die Numerische Simulation von Hochfrequenz-Schaltungen” (No. 03GUNAVN).

References

[1] Brachtendorf, H. G.; Laur, R.: Multi-rate PDE methods for high Q oscillators. in: Mastorakis, N. (ed.): Problems in Modern Applied Mathematics. CSCC 2000, MCP 2000, MCME 2000 Multi-conference, Athens, July 2000. World Scientific 2000, 391–398.

[2] Brachtendorf, H. G.; Welsch, G.; Laur, R.; Bunse-Gerstner, A.: Numerical steady state analysis of electronic circuits driven by multi-tone signals. Electrical Engineering 79 (1996), 103–112.

[3] Brachtendorf, H. G.; Welsch, G.; Laur, R.: A novel time-frequency method for the simulation

of the steady state of circuits driven by multi-tone signals. IEEE International Symposium on Circuits and Systems 9 (1997), 1508–1511.

[4] Brachtendorf, H. G.; Welsch, G.; Laur, R.: A time-frequency algorithm for the simulation of the initial transient response of oscillators. Proceedings of 1998 IEEE International Symposium on Circuits and Systems (1998), 296–299.

[5] Chua, L. O.; Ushida, A.: Algorithms for computing almost periodic steady-state response of nonlinear systems to multiple input frequencies. IEEE Trans. CAS 28 (1981) 10, 953–971.

[6] Estèvez Schwarz, D.; Tischendorf, C.: Structural analysis for electric circuits and consequences for modified nodal analysis. Int. J. Circ. Theor. Appl. 28 (2000), 131–162.

[7] Günther, M.; Feldmann, U.: CAD based electric circuit modeling in industry I: Mathematical structure and index of network equations. Surv. Math. Ind. 8 (1999), 97–129.

[8] Günther, M.; Feldmann, U.; ter Maten, E.J.W.: Modeling and discretization of circuit problems. in: Schilders, W.H.A.; ter Maten, E.J.W. (eds.): Handbook of Numerical Analysis. Special Volume Numerical Analysis of Electromagnetism. Elsevier North Holland, Amsterdam, 2005, 523–659.

[9] Hairer, E.; Nørsett, S. P.; Wanner, G.: Solving Ordinary Differential Equations. Vol. 1: Nonstiff Problems. (2nd ed.) Springer, Berlin, 1993.

[10] Hairer, E.; Wanner, G.: Solving Ordinary Differential Equations. Vol. 2: Stiff and Differential-Algebraic Equations. (2nd ed.) Springer, Berlin, 1996.

[11] Houben, S.H.M.J.: Simulating multi-tone free-running oscillators with optimal sweep following. in: Schilders, W.H.A.; ter Maten, E.J.W.; Houben, S.H.M.J. (eds.): Scientific Computing in Electrical Engineering. Mathematics in Industry 4, Springer, Berlin, 2004, 240–247.

[12] Horneber, E. H.: Analyse nichtlinearer RLCÜ-Netzwerke mit Hilfe der gemischten Potentialfunktion mit einer systematischen Darstellung der Analyse nichtlinearer dynamischer Netzwerke. PhD thesis, University Kaiserslautern, 1976.

[13] Kampowsky, W.; Rentrop, P.; Schmitt, W.: Classification and numerical simulation of electric circuits. Surv. Math. Ind. 2 (1992), 23–65.

[14] Knorr, S.; Günther, M.: Index analysis of multirate partial differential-algebraic systems in RF-circuits. in: Anile, A.M.; Alì, G.; Mascali, G. (eds.): Scientific Computing in Electrical Engineering. Mathematics in Industry 9, Springer, Berlin, 2006, 93–100.

[15] Knorr, S.; Feldmann, U.: Simulation of pulsed signals in MPDAE-modelled SC-circuits. in: Di Bucchianico, A.; Mattheij, R.M.M.; Peletier, M.A. (eds.): Progress in Industrial Mathematics at ECMI 2004. Mathematics in Industry 8, Springer, Berlin, 2006, 159–163.

[16] Kundert, K. S.; Sangiovanni-Vincentelli, A.; Sugawara, T.: Techniques for finding the periodic steady-state response of circuits. in: Ozawa, T. (ed.): Analog methods for computer-aided circuit analysis and diagnosis, New York, 1988, 169–203.

[17] Lang, B.: Einbettungsverfahren für Netzwerkgleichungen. PhD thesis, University Bremen, Shaker, Aachen, 2002.

[18] Lehtovuori, A.; Virtanen, J.; Valtonen, M.: GMRES preconditioner for multivariate steady-state time-domain method. Proceedings of IMS'2003, Philadelphia, 8-13 June, 2003, 2129–2132.

[19] Narayan, O.; Roychowdhury, J.: Analyzing oscillators using multitime PDEs. IEEE Trans. CAS I, 50 (2003), 894–903.

[20] Ngoya, E.; Larcheveque, R.: Envelop transient analysis: a new method for the transient and steady state analysis of microwave communication circuits and systems. IEEE Microwave Theory and Techniques Symposium Digest, June 1996, 1365–1368.

[21] Pulch, R.; Günther, M.: A method of characteristics for solving multirate partial differential equations in radio frequency application. Appl. Numer. Math. 42 (2002), 397–409.

[22] Pulch, R.: Finite difference methods for multi time scale differential algebraic equations. Z. Angew. Math. Mech. 83 (2003) 9, 571–583.

[23] Pulch, R.: A parallel finite difference algorithm for multirate partial differential algebraic equations. in: Antreich, K.; Bulirsch, R.; Gilg, A.; Rentrop, P. (eds.): Modeling, Simula-

tion and Optimization of Integrated Circuits. International Series of Numerical Mathematics Vol. 146, Birkhäuser, Basel 2003, 153–166.

[24] Pulch, R.: Multi time scale differential equations for simulating frequency modulated signals. Appl. Numer. Math. 53 (2005) 2-4, 421–436.

[25] Pulch, R.: Warped MPDAE models with continuous phase conditions. in: Di Bucchianico, A.; Mattheij, R.M.M.; Peletier, M.A. (eds.): Progress in Industrial Mathematics at ECMI 2004. Mathematics in Industry 8, Springer, Berlin, 2006, 179–183.

[26] Pulch, R.: Semidiscretisation methods for warped MPDAEs. in: Anile, A.M.; Alì, G.; Mascali, G. (eds.): Scientific Computing in Electrical Engineering. Mathematics in Industry 9, Springer, Berlin, 2006, 101–106.

[27] Pulch, R.: Variational methods for solving warped multirate partial differential algebraic equations. submitted to: SIAM Journal on Scientific Computing.

[28] Roychowdhury, J.: Efficient methods for simulating highly nonlinear multi-rate circuits. Design Automation Conference (1997), 269–274.

[29] Roychowdhury, J.: Analysing circuits with widely-separated time scales using numerical PDE methods. IEEE Trans. CAS I 48 (2001) 5, 578–594.

[30] Ho, C. W.; Ruehli, A. E.; Brennan, P. A.: The modified nodal approach to network analysis. IEEE Trans. CAS 22 (1975), 505–509.

[31] Simeon, B., Arnold, M.: Coupling DAE's and PDE's for simulating the interaction of pantograph and catenary. Math. and Computer Model. of Systems 6 (2000), 129–144.

[32] Striebel, M.: Hierarchical Mixed Multirating for Distributed Integration of DAE Network Equations in Chip Design. PhD thesis, to appear in: VDI-Verlag, Düsseldorf, 2006.

[33] Tischendorf, C.: Topological index calculation of differential-algebraic equations in circuit simulation. Surv. Math. Ind. 8 (1999), 187–199.

[34] Ushida, A.; Chua, L. O.: Frequency-domain analysis of nonlinear circuits driven by multitone signals. IEEE Trans. CAS 31 (1984) 9, 766–779.

[35] Zhu, L. L.; Christoffersen, C. E.: Fast transient analysis of oscillators using multiple time scales with accurate initial conditions. IEEE Canadian Conference on Computer and Electrical Engineering Digest, Saskatoon, May 2005, 700–703.

[36] Zhu, L. L.; Christoffersen, C. E.: Adaptive harmonic balance analysis of oscillators using multiple time scales. 3rd International IEEE Northeast Workshop on Circuits and Systems Digest, June 2005, 187–190.